

THOMPSON RIVERS UNIVERSITY
Undergraduate Physics Program

TIGRESS ARRAY OVERVIEW
and
OTHER PROJECTS

Performed At
TRIUMF
4004 Wesbrook Mall
Vancouver, BC

by
Owen Paetkau
T00034990

WORK TERM REPORT
May - August 2015

in partial fulfillment of the requirement for the
BACHELOR OF SCIENCE

Submitted August 26th, 2015

The TIGRESS array is used for gamma ray spectroscopy in the ISAC II hall of TRIUMF. It is often used in conjunction with other detectors for gamma ray detection. The lifetimes and energies of excited nucleus states releasing gamma rays can help to describe the shape of the nucleus and its interactions with other nuclei. Throughout a beam time, there are several experiments completed. During the summer of 2015, a TIP (TRIUMF Integrated Plunger) and a SHARC (Silicon Highly-segmented Array for Reactions and Coulex) experiment were completed. During these experiments, I helped set up the TIGRESS array in proper configuration and assisted on beam shifts.

Along with experiments, there were many side projects that are required for maintenance and further development of the detectors and the array itself. This report will describe projects completed on commissioning the CAEN multi-channel analyzer (MCA), cross talk testing for a future data acquisition system (DAQ) and testing and simulating the TRIUMF Bragg (TBragg) detector. All of these projects were side projects that I completed between (or during) experiments.

Contents

List of Figures and Tables	4
1 Introduction	5
2 Experimentation	6
2.1 TIGRESS Array	6
2.2 TIP Experiment	8
2.3 SHARC Experiment	9
3 Projects	10
3.1 CAEN Multi-Channel Analyzer	11
3.2 Cross Talk Testing	19
3.3 TBragg Simulations	22
4 Conclusion	27
References	28

List of Appendices

Appendix I - SCSI Connections and Cable Cross Talk Images ..	29
Appendix II - Coaxial Cables Cross Talk Images	41

List of Figures and Tables

2.1.1. Segmentation of the HPGe crystals. Each detector has a total of 40 signals which are all sent to the DAQ to be read for events.

2.1.2. Half of the TIGRESS array with the suppressors pulled back. The segmentation on each detector is made clear by the colouring on the crystals.

3.1.1. Basic MC² Analyzer software interface. The main features to observe are the acquisition setup, the spectra list, the signal interface and the region of interest (ROI) editor.

3.1.2. The settings when using the waveform to mimic gamma ray decays on the germanium detectors. From top to bottom; a) input signal, b) trigger and c) energy filter settings.

3.1.3. Calibrated pulses received from the waveform generator. The 50mV, 100mV, and 150mV have been calibrated as 500keV, 1000keV and 1500keV respectively.

3.1.4. Settings used for the GRIFFIN 10 detector with a ⁶⁰Co source beneath the detector. From top to bottom; a) the input signal, b) trigger, and c) energy filter settings.

3.1.5. Peaks created from the ⁶⁰Co source as determined by the MCA. The three peaks are the 1173keV and 1332keV lines from ⁶⁰Co and the 1460keV line from potassium. The bottom portion of the figure indicates the FWHM and peaks of the selected regions of interest.

Table 3.1.1. Reproducibility trials with flat top time of 1.0 μ s and rise time of 4.5 μ s.

Table 3.1.2. Values from the FWHM of the 1332keV peak during varied flat top and rise times.

3.2.1. The experimental setup used to determine cross talking within the SCSI and coaxial cables.

3.2.2. SCSI connections with cables used in the cross talk testing.

3.2.3. Coaxial cable used to test cross talking for the new data acquisition system.

3.3.1. Bragg curve created by the SRIM software for ²⁰Ne at 99MeV. The peak is apparent and has a high Z dependence which is useful in particle identification.

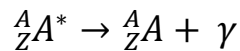
3.3.2. A sample particle identification plot from simulation with the short filter value plotted on the y axis and the long filter value on the x axis. This is a series of energies from 6.05MeV/u to 8.00 MeV/u for ²⁸Si at 950 torr (ie., 0.001944g/cm³ in SRIM simulation).

3.3.3. Spectrum of ²⁸Si with a working chamber length of 10.00cm. The energy series runs from 8.00MeV/u to 0.00MeV/u in a pressure of 950torr.

3.3.4. Data taken using the TBragg during the S1554 SHARC experiment. The large spot indicates ²⁸Si within the beam. This image compares well to Figure 2 due to the length of the tail.

1 – Introduction

The TIGRESS (TRIUMF ISAC Gamma Ray Escape Suppressed Spectrometer) is located in the ISAC II hall of TRIUMF on the southern campus of UBC. The array itself is used in conjunction with other, smaller detectors for gamma ray spectroscopy. These other detectors will allow for detailed detection of gamma decays. Gamma decays occur when an excited nucleus releases a high energy photon to return to its ground state. The equation below is used to describe a gamma decay.



The photon released can have many energy levels and in the same way that electrons have quantized energy levels, the nucleus of an atom also has quantized energy levels. The energy levels and their separation depend on the total angular momentum and parity. The model used to describe these energy levels is based on the shell model which has similar s/p/d/f shell orbitals as the electron orbitals.

Gamma ray spectroscopy at TRIUMF relies on spectra, effective DAQ and beam composition. All three of these aspects require maintenance as well as further innovation. This report will cover a project on each of these aspects. The CAEN MCA being commissioned will be used in detector testing in the TIGRESS detector lab. This report will give a detailed introduction to many aspects of the analyzer software plus a couple tests completed for optimization of the signal resolution. The cross talk tests completed on SCSI connectors and cables will give insight into the future TIGRESS DAQ. This will examine both the SCSI connectors and cables to determine if their cross talk effect is significant compared to the signals being examined. Finally, the TBragg simulations and testing will allow for more effective beam analysis. It will help determine the composition of a beam as well as give more insight into the TBragg detector itself.

2 – Experimentation

For gamma ray spectroscopy to occur, the isotopes must already be in an excited state. In the case of most of the experiments, there is some apparatus attached to the detector that aids in the excitement of the nucleus. In this case, the TIP experiment used fusion evaporation reactions to excite the nucleus while the SHARC experiment used (d,p) reactions to create an excited state.

2.1 – TIGRESS Array

The whole array itself consists of a maximum of 16 high purity germanium (HPGe) detectors. These HPGe crystals are segmented in such a way to give a better idea of the location of gamma decays. The clovers each consist of four HPGe crystals which are each segmented into 8 parts. This segmentation allows for better measurement of the energies and angles of the gamma rays emitted from the decay. As seen in Figure 2.1.1, the segmentation creates 8 signals from each crystal plus two signals from the crystal cores. This creates a total of 40 signals output from each HPGe detector. In addition to the HPGe detectors, there are Compton suppression shields attached to each detector. As can be seen in Figure 2.1.2, there are four inner shields attached directly to the clovers themselves plus another four outer shields. In the figure the outer shields have been set to a pulled back position so the array might be seen. These Compton shields add another aspect of kinematics calculations and detection of any stray gamma rays. Each of the suppression shields contributes around 5 signals to the output.

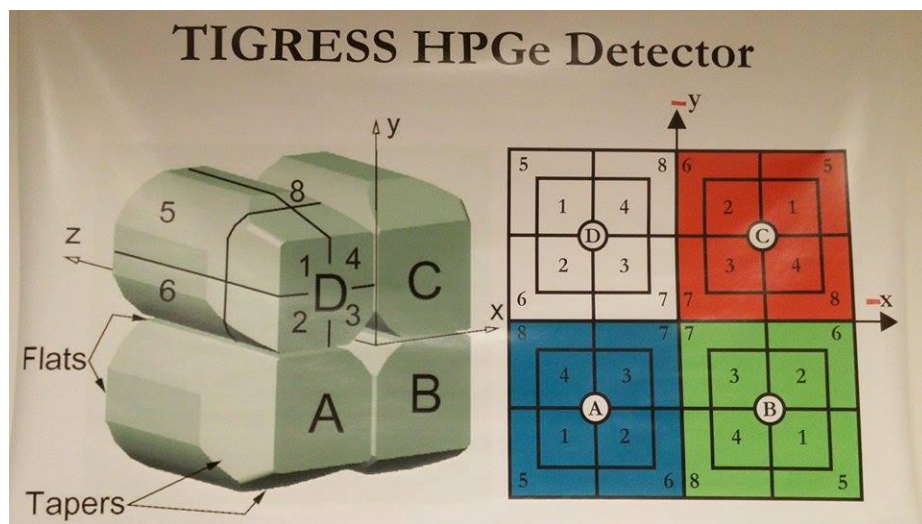


Figure 2.1.1. Segmentation of the HPGe crystals. Each detector has a total of 40 signals which are all sent to the DAQ to be read for events.

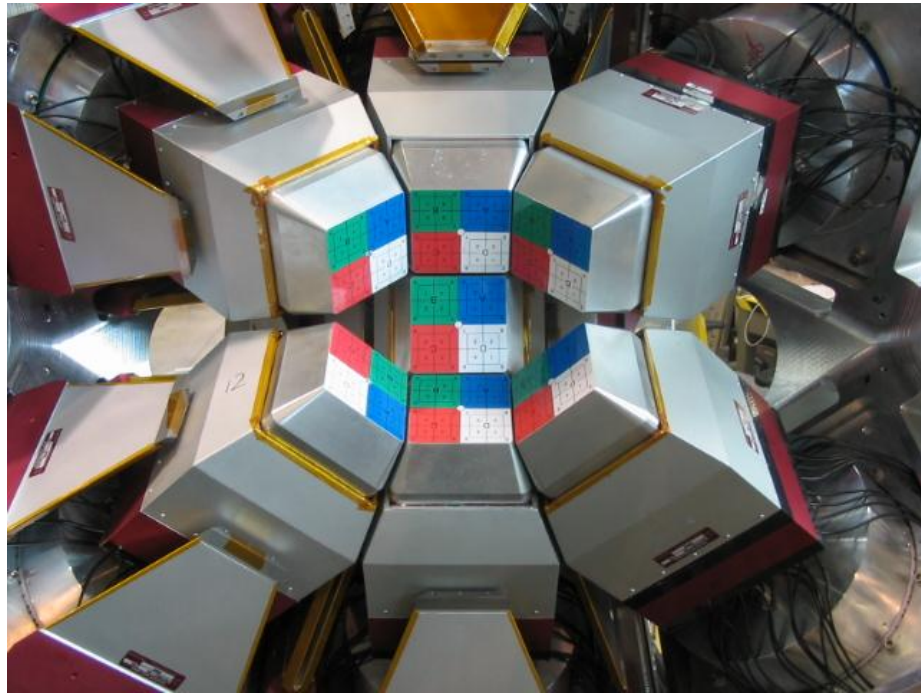


Figure 2.1.2. Half of the TIGRESS array with the suppressors pulled back. The segmentation on each detector is made clear by the colouring on the crystals.

Once these signals have been created, they need to be collected. The data acquisition system (DAQ) at TIGRESS consists of several levels of collection and data sorting. The first level, dubbed the TIG10s, collect all of the signals from the various channels. These TIG10s are the red modules within the shack that have ten channels. If any of the collected signals is seen as an event (a gamma decay), then it is sent to a new set of cards. These cards are called Master cards and they take several events and determine if they are above the threshold for an actual gamma decay. There is a lot of background radiation and eliminating this using threshold triggers within the cards will facilitate the sorting process. Once a signal has passed this step, it is stored as an event. Each channel has its own spectrum within the roody software. There is also a hit pattern and a cumulative spectrum, both of which are useful in troubleshooting channels.

2.2 – TIP Experiment

The TRIUMF Integrated Plunger (TIP) experiment was commissioned in May 2015 with the first radioactive experiments as well as several non-radioactive experiments. The TIP device was manufactured by SFU and the group there manages the project. The device is based on a nuclear physics experimental technique using a plunger. The plunger is used to measure the lifetime of a nuclear excited state. The plunger apparatus itself consists of a stopping foil and a target foil which are a variable distance apart. The stopping foil is made of a dense material, such as lead, so the beam is completely stopped within the foil. This stopping foil is on a motor that allows it to approach the target foil to within a distance as small as 10 µm. The target foil is used to excite the isotope that passes through it and thus it is thin. The material used in the target foil depends on the beam composition. Once the nucleus has been excited, it then travels between the target and stopper foil before stopping within the stopping foil. Throughout this process, the gamma decay is measured. Due to the Doppler shift, gamma decays in flight will exhibit a different energy compared to stopped decays. Using this effect, spectrums of these gamma decays can be taken at several different distances which allows for the creation of a decay curve. The lifetime of a given excited state can be determined from analysis of this curve.

The TIP device works on the plunger technique described above. The device has been designed to fit directly in the TIGRESS array so that it may be used in conjunction with the HPGe clover detectors. The plunger itself excites the nuclei of the beam by using a method called fusion evaporation. Fusion evaporation works due to an initial collision between two elements, these elements then combine before undergoing an evaporation process. This evaporation process preferably emits neutrons and thus leaving a neutron deficient nucleus. Once the neutron has been emitted, an excited nucleus is left behind for further experimentation.

A series of three piezo electric motors are used on the TIP device to rotate the target foil. Ideally, this foil should be perpendicular to the stopper foil. Thus the piezo electric motors are used to place the foils as perpendicular as possible to each other. To test how perpendicular the foils are, a measurement of the capacitance between the target and stopper foil is taken. This measurement is maximized as this is the point that the foils are most perpendicular. A computer program moves each motor in slight steps, keeping the mean distance between the foils the same but rotating the plane of the target foil. Once the capacitance is at a maximum, this location is saved and returned to the user as the most perpendicular point. Having the plates as perpendicular as possible is crucial for Doppler shift measurements as well as determining the distance between the plates.

2.3 – SHARC Experiment

The SHARC (Silicon Highly-segmented Array for Reactions and Coulex) detector is a series of silicon detectors and sits in the beamline of the TIGRESS array. These silicon detectors sit around the beam and detect gamma decays to a higher precision with more collision information. This highly-segmented array along with the TIGRESS array allows for high precision counts and kinematics calculations.

Experiment S1554 was aimed to use a (d,p) reaction with a beam of ^{28}Mg at an energy of around 8MeV/u. The purpose was to explore the structure in the exotic region around the island of inversion. This would be achieved due to the fact that the reaction populates excited energy states of ^{29}Mg . The energies and angles of the gamma rays provide enough information to determine the energy levels that the neutrons fall into in the new nucleus. As described in the TBragg Simulation section, there was some beam contamination throughout the experiment, causing the beam to be composed of mostly ^{28}Si . Thus this experiment was not properly completed.

3 - Projects

During my time at TRIUMF, there were several side projects to work on while the experiments were ongoing or during downtime between experiments. The first of these projects was commissioning the CAEN multi-channel analyzer. This project was done to become familiar with the software as well as understand the workings of the digital analyzer. By using a pulsar to simulate germanium detector signals, a spectrum could be worked with as well as determining the most effective parameters.

The second project was testing SCSI and coaxial cables and connections for cross talk. Cross talk occurs when signals from one cable interact with another cable to create a false signal. This happens most often in connections but can also occur in the cable itself. This project was to test different cables and connections to determine the combination with the least cross talk that would be most effective for a new TIGRESS data acquisition system to replace the current SCSI based system.

The final project was working on simulations to create particle identification plots for the TBragg detector. The TBragg is an ionization chamber dubbed TBragg for TRIUMF Bragg detector. It is a diagnostic device used to determine beam composition. Simulations, completed using SRIM and a C++ code, were used to quantify data results seen from the TBragg detector itself.

3.1 - CAEN Multi-Channel Analyzer

The DT5781 CAEN Multi-Channel Analyzer (MCA) is a four input, spectrum analysis device that runs with the MC² Analyzer software. This software is available for download from the CAEN website with a CAEN account. The MC² Analyzer is able to create basic histograms for all four channels, calibrate with specific energies, describe regions of interest, as well as handle all of the settings for the MCA. The MC² Analyzer User Manual (UM3182 on the CAEN website [1]) has a detailed description of how to create a proper input signal, how to calibrate the spectrum, saving the selected data as well as some troubleshooting tips. This report will describe the results from basic testing on the CAEN digital MCA and compare it to tests from the ORTEC analog MCA.

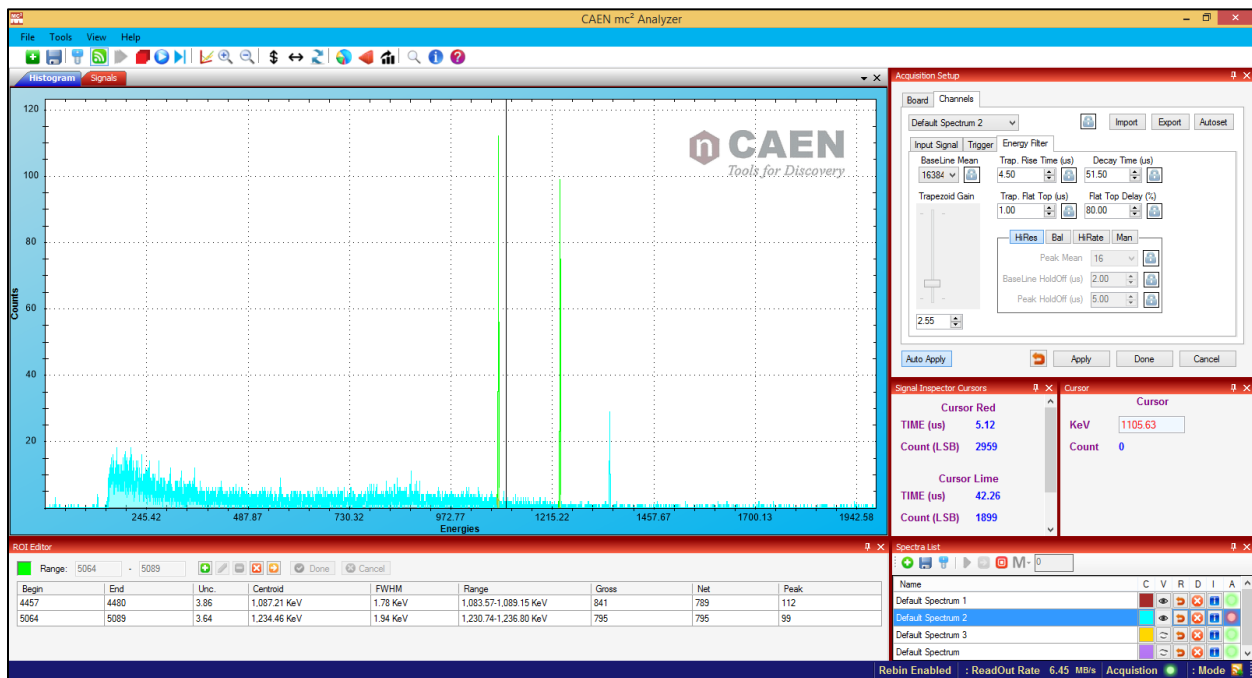


Figure 3.1.1. Basic MC² Analyzer software interface. The main features to observe are the acquisition setup, the spectra list, the signal interface and the region of interest (ROI) editor.

1. Graphical User Interface

The first step is to become familiar with the MC² Analyzer software. To upload a device or a spectrum, use the green plus in the upper left hand corner of the toolbar. This will bring up a window asking to select a device. There is no need to change any of the options here, just hit connect and the software should recognize the DT5781 MCA. If the device is not recognized, ensure that the USB drivers have been installed from the CAEN website (<http://caen.it/jsp/Template2/CaenProd.jsp?parent=64&idmod=922>). Once the spectra are

active, there should be a spectra list as seen in the bottom right hand corner of Figure 1. To set the device up for data acquisition, the acquisition setup window can be found on the toolbar as a key or around the outside of the histogram. This window has all of the settings that will affect the resolution and data acquisition. Beginning with the input signal tab, it is important to select the correct pulse polarity as the MCA will analyze it accordingly. For the GRIFFIN and TIGRESS germanium gamma ray detectors, the pulse is negative. This device uses a trapezoidal energy filter to determine the location of the peaks and thus it is easiest to send the signal directly from the detector to the MCA. There is no need for any signal analysis or change before the MCA itself. The setup of the trigger and energy filter tabs is described in detail within the MC² Analyzer User Manual [1, pp. 32-40]. Once the acquisition setup is complete, regions of interest can be examined or used in an energy calibration. This process can also be found in depth within the software user manual [1, pp. 43-46].

2. Pulser Test

The first tests completed on the CAEN MCA were with a pulser. The waveform generator created pulses resembling gamma decays within the germanium detectors to best mimic testing with a detector. However, the waveform was set to 14 MSa/s which is a much larger signal than a germanium detector may receive. The amplitudes of the pulses were set at 50mV, 100mV and 150mV. The settings in Figure 3.1.2 had the 100mV peak appear at around the 4000 channel. To adjust the position of the peaks, the trapezoidal gain is the most useful tool for shifting peaks from side to side. These tests resulted in peaks at 2000, 4000 and 6000 with about a FWHM of 0.5keV. This high resolution is to be expected as the pulses are ideally perfectly uniform from the waveform generator. An example of the three peaks seen from the waveform generator is displayed in Figure 3.1.3. This figure also displays calibrated energies. Energy calibrations can be completed by selecting a region of interest and activating the calibration window under tools or by hitting F7. Taking the centroid of a region of interest and setting the proper energy will effectively calibrate the curve. As with most calibrations, two samples need to be entered for an effective calibration.

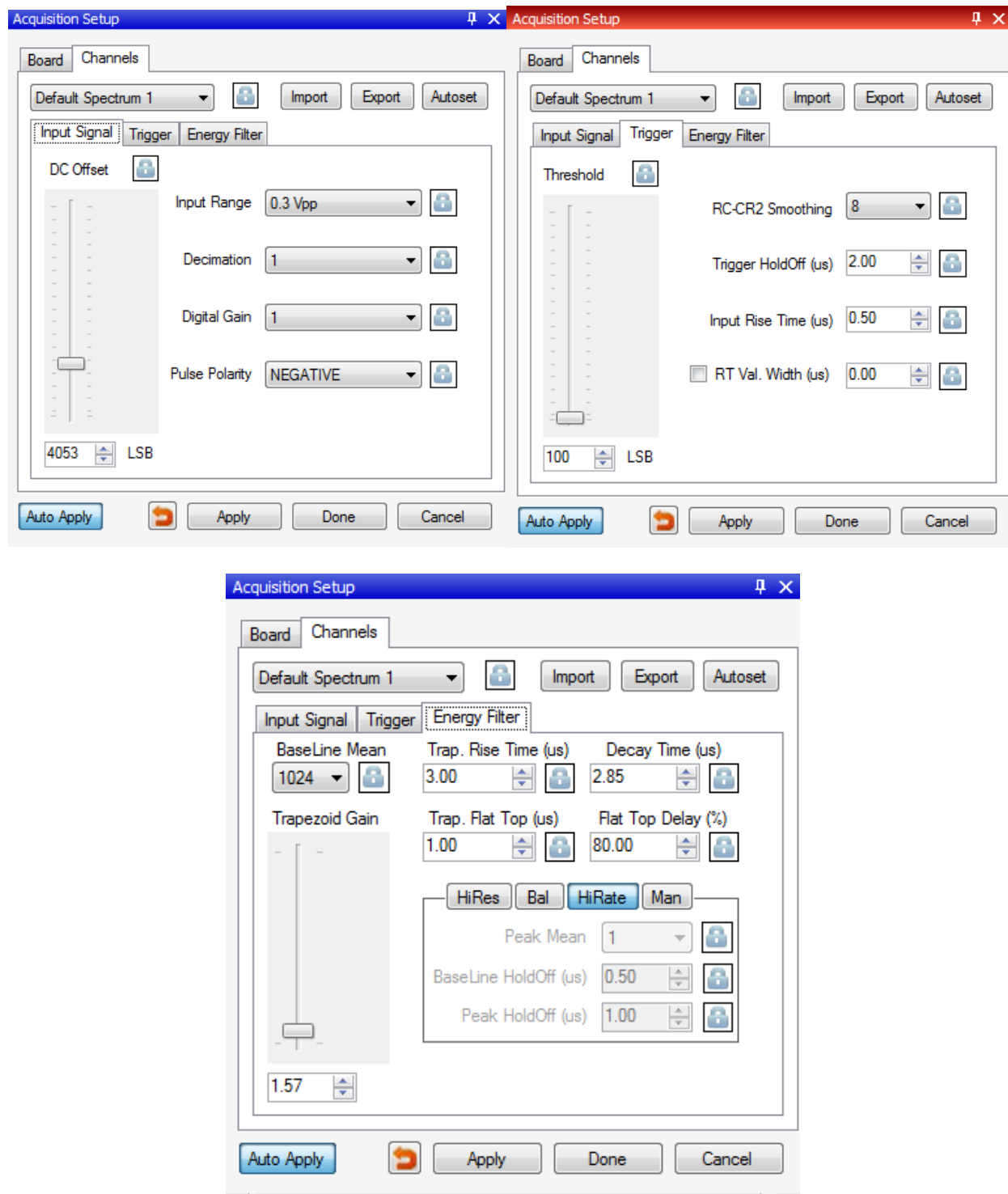


Figure 3.1.2. The settings when using the waveform to mimic gamma ray decays on the germanium detectors. From top to bottom; a) input signal, b) trigger and c) energy filter settings.

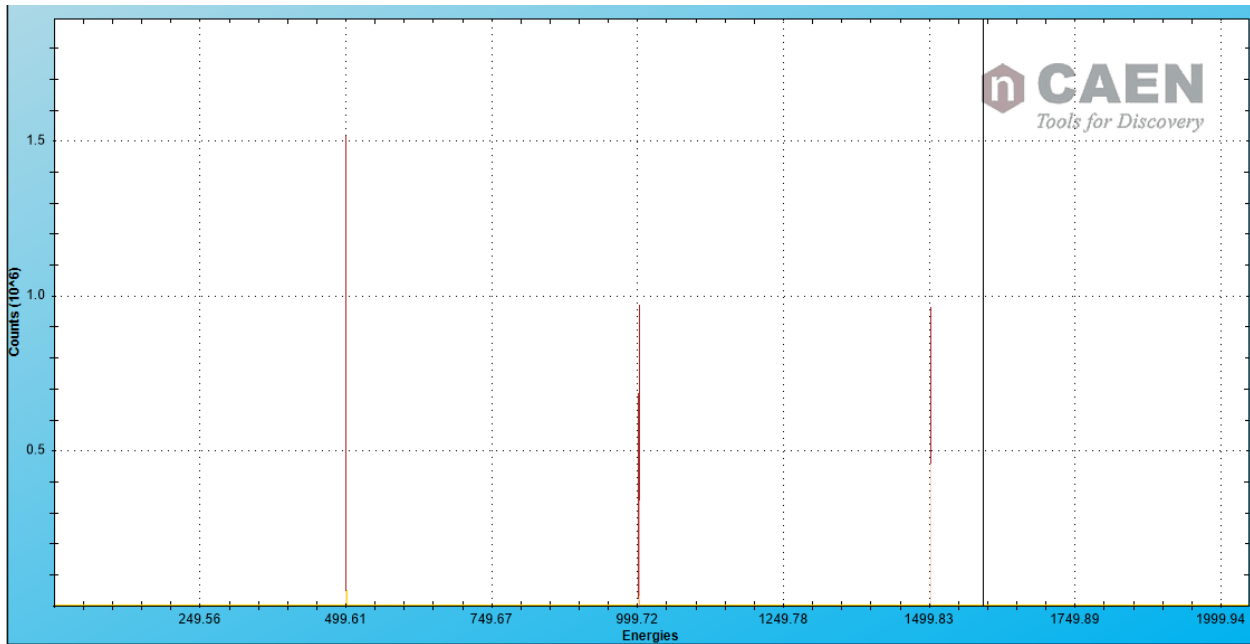


Figure 3.1.3. Calibrated pulses received from the waveform generator. The 50mV, 100mV, and 150mV have been calibrated as 500keV, 1000keV and 1500keV respectively.

3. Setup with GRIFFIN Clover

Once the calibration tests with the waveform generator were complete, the MCA was used to describe signals from the GRIFFIN 10 detector currently undergoing maintenance (see HPGe Detector ELOG 13/05/2015). The settings of this analyzer needed to be completely reconfigured to match the signal from the detector. As mentioned before, there is no need to put the detector signal through a waveform analyzer as there is an energy filter built into the CAEN MCA. Following the process within the MC² Analyzer Software Manual will be the most effective method of determining the proper settings [1, pp. 28-40]. Figure 3.1.4 indicates the settings used when determining the peaks and FWHM of a ⁶⁰Co source. Compared to the waveform generator, the decay time has increased substantially along with the baseline mean while the other values are similar. The threshold has also been increased by quite a bit but this is subject to change depending on the level of background noise that is seen in the signal. Subsequently, Figure 3.1.5 indicates a trial spectrum completed in channel 3 of the MCA. Each channel acts slightly differently and has their own calibration but the values from each peak are within 5keV of each other. The two red peaks are the regions of interest as described at the bottom of the screen. Upon completing a calibration, the FWHM is around 2keV for both peaks.

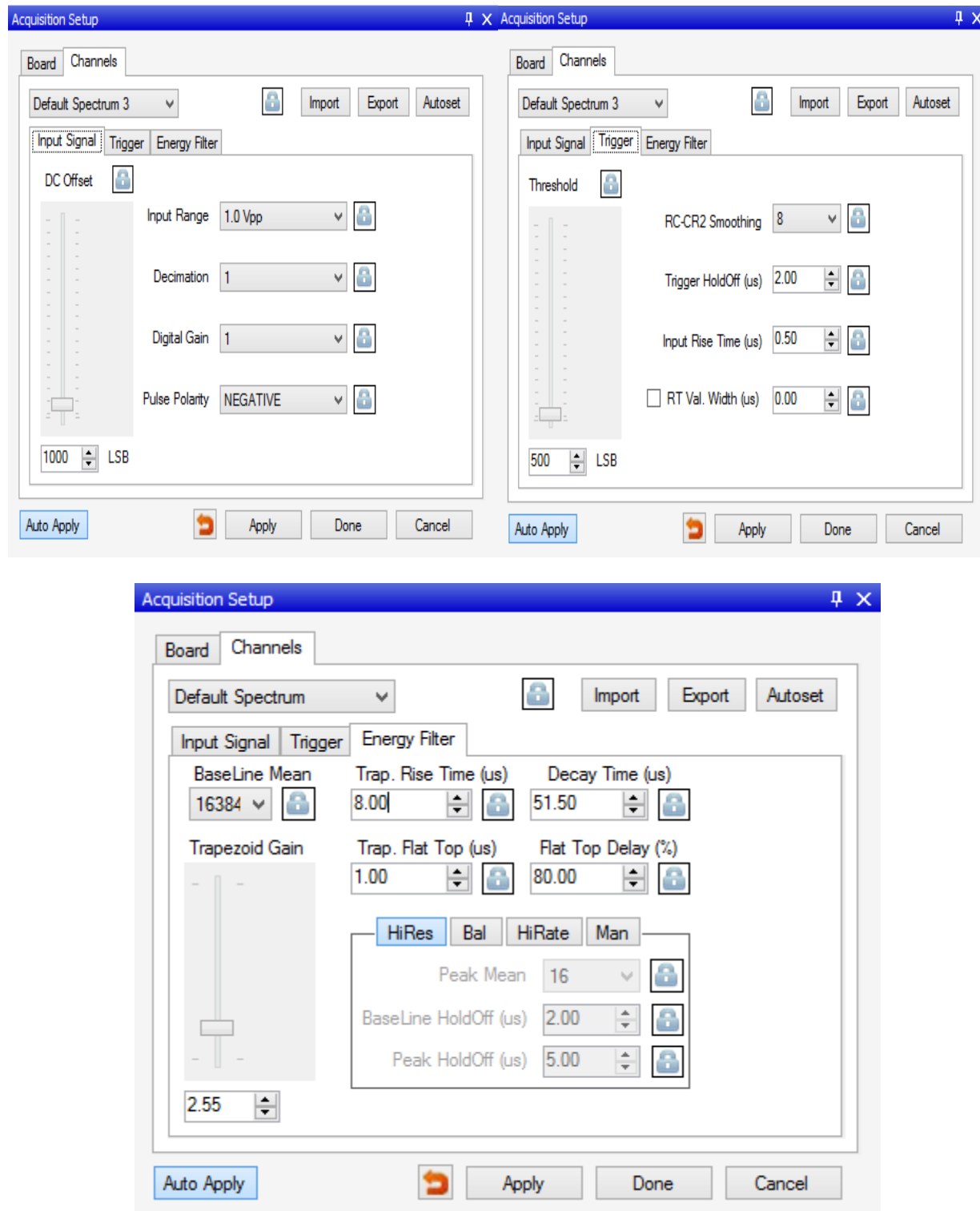


Figure 3.1.4. Settings used for the GRIFFIN 10 detector with a ^{60}Co source beneath the detector.
From top to bottom; a) the input signal, b) trigger, and c) energy filter settings.

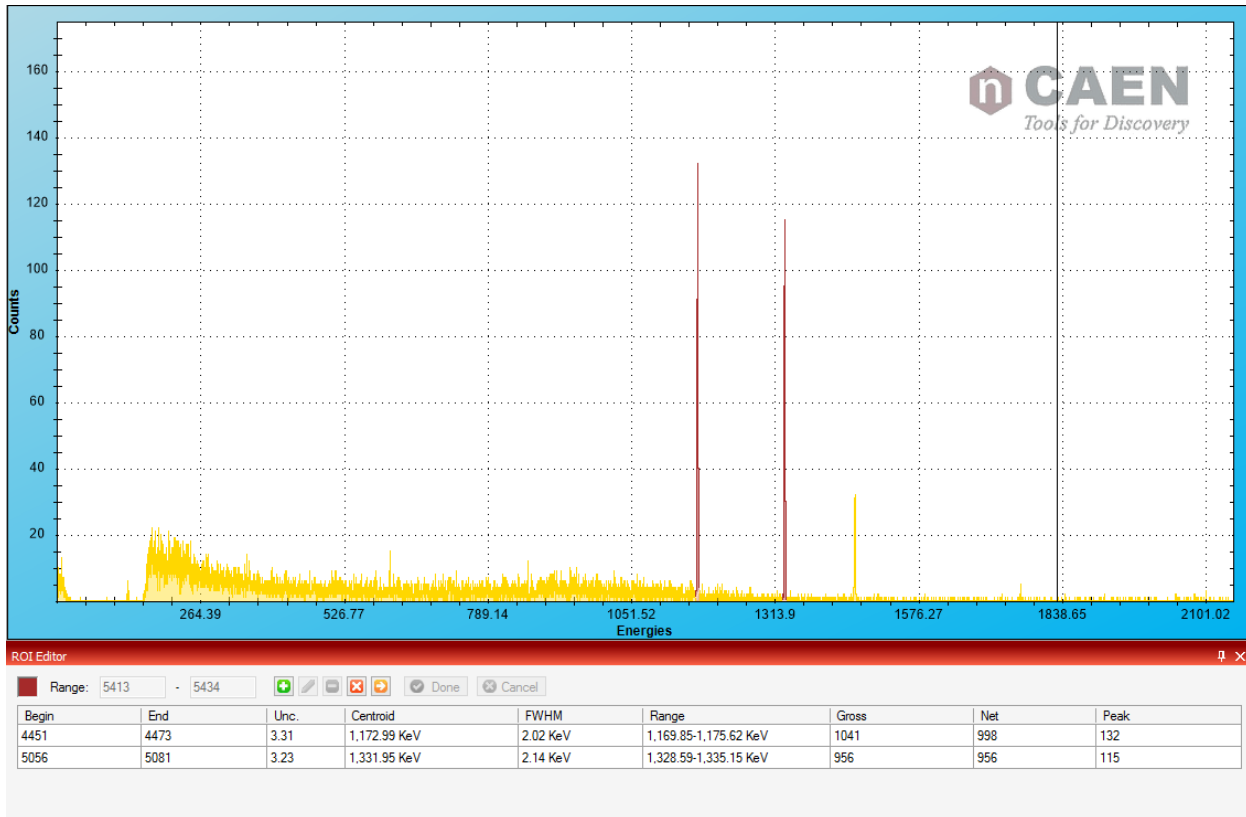


Figure 3.1.5. Peaks created from the ^{60}Co source as determined by the MCA. The three peaks are the 1173keV and 1332keV lines from ^{60}Co and the 1460keV line from potassium. The bottom portion of the figure indicates the FWHM and peaks of the selected regions of interest.

To determine the reproducibility of the CAEN DT5781 MCA, 5 trials were completed with the white crystal of GRIFFIN 10. These trials consisted of 10 000 data points per peak with the energy filter set to a trapezoidal rise time of 4.5 μs and a trapezoidal flat top time of 1.0 μs . The FWHM of the 1332keV peak was determined using fitting parameters within excel. The following equation was used as the basis with varying A, B, C, and D to correctly fit the Gaussian curve.

$$f(x) = Ae^{\frac{-(x-B)^2}{2C^2}} + D$$

All of the 1332keV peaks were analyzed using this fitting equation within excel. Table 3.1.1 indicates the values determined from the reproducibility tests.

Table 3.1.1. Reproducibility trials with flat top time of 1.0 μ s and rise time of 4.5 μ s.

Trial	1173keV Peak FWHM (keV)	1332keV Peak FWHM (keV)
1	1.935492	1.962159
2	1.909741	1.970073
3	1.928407	2.011969
4	1.899974	1.972479
5	1.929818	2.000739

Optimization trials were completed in an attempt to decrease the FWHM values, increasing the resolution of each peak. These trials were completed on the white crystal of the GRIFFIN 10 detector in the TIGRESS lab for repairs. Each trial consists of at least 10 000 data points per peak to create a proper statistical analysis. To optimize the resolution, the trapezoidal flat top time and rise time were varied. Due to the nature of the trapezoidal energy filter, these values were most effective in fine tuning the resolution of the signal. These settings could vary depending on the conditions of the room. For example, when the liquid nitrogen was refilling the detector, the resolution measurements were worse compared to otherwise. The vibration caused enough background noise to skew the measurements. Two points (6, 0.5 / 6, 1.0) were taken a second time to determine the proper FWHM as they appeared extremely skewed, potentially due to the liquid nitrogen. The data in Table 3.1.2 indicates the 30 trials completed in an attempt to optimize the trapezoidal filter settings.

Table 3.1.2. Values from the FWHM of the 1332keV peak during varied flat top and rise times.

Trapezoidal Rise Time (μ s)	Trapezoidal Flat Top Time (μ s)				
	0.5	1	1.5	2	2.5
2	2.286159	2.232092	2.258284	2.357681	2.236214
3	2.113531	2.072628	2.08214	2.106343	2.088387
4	2.048139	2.0272	1.983025	2.054763	2.072815
6	1.960973/ 1.956963	2.225495/ 1.908355	1.965617	1.950382	1.941478
8	1.915623	1.874963	1.893551	1.876542	1.899441
10	1.895146	1.93572	1.974927	2.040764	2.089654

The resolution of the CAEN DT5781 MCA has a variation of 0.04keV depending on the trial. This is approximately a 2% effect and is very small compared to the FWHM observed in the trials. This variation is not large enough to affect the validity of the FWHM values determined within experimentation. These trials were also taken with values that varied from the optimized values and this could cause some error. After the optimization trials, the settings that create the best resolution occur when the trapezoidal rise time is 8 μ s. The values when the trapezoidal flat top times are 1.0 μ s and 2.0 μ s are very similar and give the best resolution. Note that these values are determined within the TIGRESS detector lab. Due to vibrations of the detector, there is potential that the optimal settings could vary depending on the environment. This holds true for conditions where the detector is being filled by liquid nitrogen.

3.2 - Cross Talk with SCSI and Coaxial Cables

Tests of the cross talk within the SCSI connections were completed prior to these tests. These tests were to determine the cross talking effect contributed by the cable transferring the data. A comparison of two cables was completed: the first cable is the SCSI cable currently in use with the TIG64 units and the second cable is the proposed coaxial cable for the new data acquisition system. Large amplitude signals or large voltage off-sets indicate a large value of cross talking between channels of the SCSI connections. These large signals could potentially send false triggers when implemented in the TIGRESS array. Thus, the cross talking needs to be minimized to decrease the number of false events being observed.

The oscilloscope images were taken using the circuit diagram as seen in Figure 3.2.1. A square wave with a peak-to-peak voltage of 1.0 V and a frequency of 1.0 kHz was input into one end of the SCSI connection and cable. This signal was also sent into a $1\text{ M}\Omega$ terminated oscilloscope channel (Channel 1). It was set to $1\text{ M}\Omega$ to correctly mimic a pre-amp. This was then properly terminated with the corresponding channel at the other end of the cable.

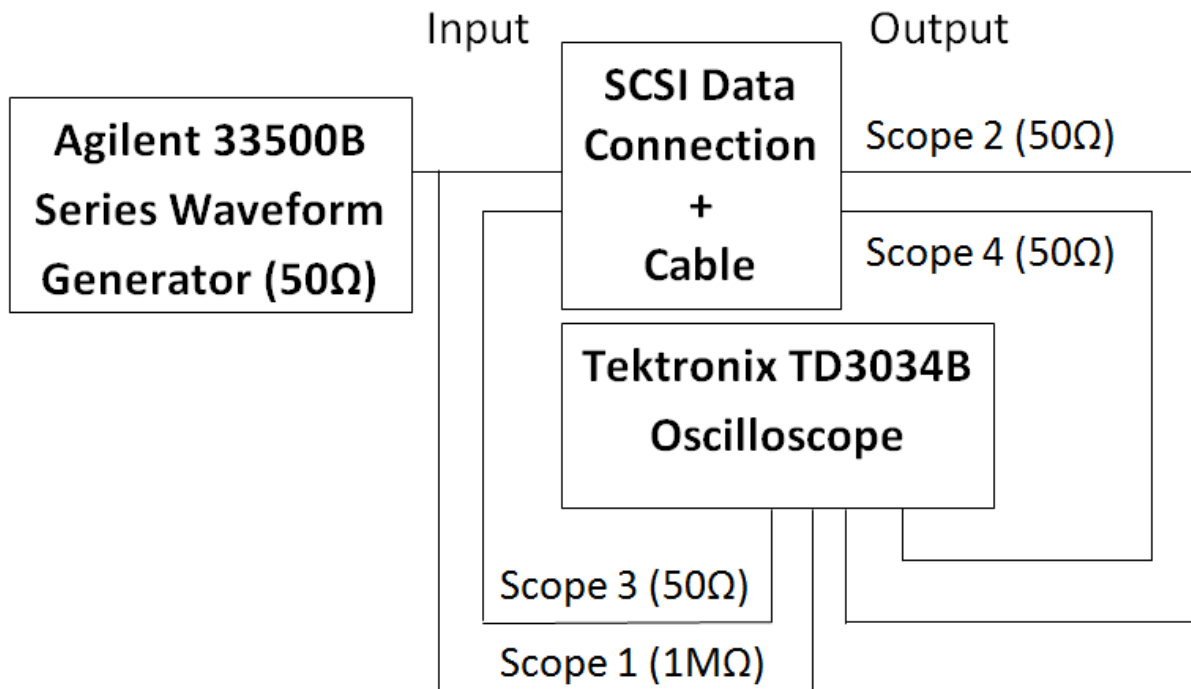


Figure 3.2.1. The experimental setup used to determine cross talking within the SCSI and coaxial cables.

SCSI Cables

Previously, there has been cross talking of around 5-10% throughout the entire system when using SCSI connections and cables. The previous tests indicated that the SCSI connections themselves only resulted in 0.5% cross talking thus the cable must contribute the majority of the cross talking. The four channels 8, 9, 24, and 25 received input and the channels nearby were tested. The SCSI connector was tested and the number of channels away from the input signal affected the cross talking effect. Each of the images below has one of the four input channels as well as a channel being tested for cross talking. The cable used in this case is displayed in Figure 3.2.2. It is a 60 foot long SCSI cable with a SCSI connector at either end. These connectors are transitioned to limo cables using the converter boards seen below.

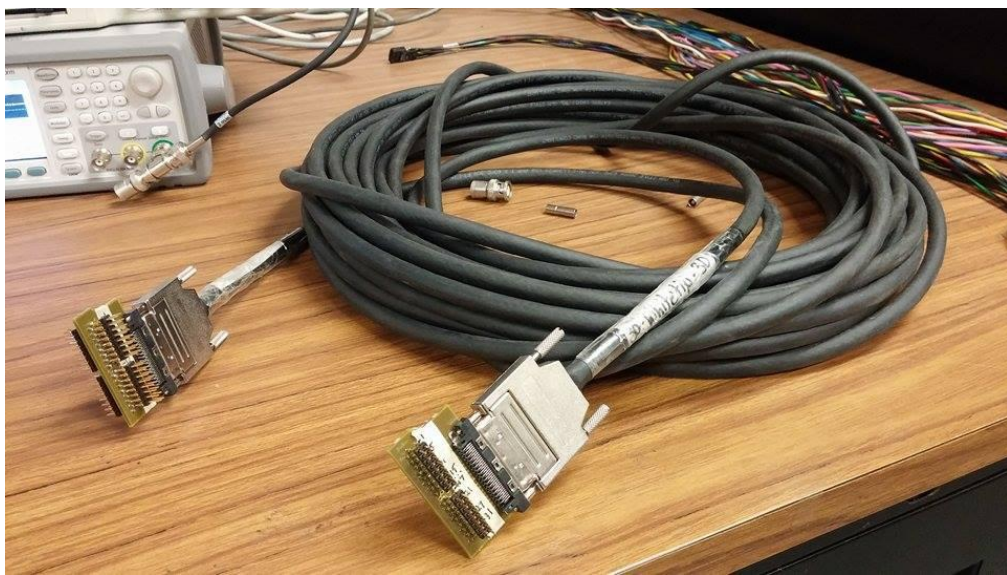


Figure 3.2.2. SCSI connections with cables used in the cross talk testing.

The images in Appendix I describe the cross talk between channels of the SCSI connector and cable. As determined in the initial SCSI connection test, the cross talk varied as a function of channels away from the input. In this case, there is not a large variation between the cross talk signals. This indicates that the channel variation occurs only within the SCSI connector itself. Note the scale on both the cross talk channels and the time. The voltage is set to a scale of 50mV while the time is set to a scale of 100ns. The input signal being tested for cross talk has an initial peak of between 50-100 mV while the output pulse has a similar inverted signal. These cross talking signals return to the baseline noise after around 2 μ s. There is also some poor termination that can be observed within the input square wave. This is due to the SCSI cable having impedance that varies from the 50 Ω expected of a transmission line. Due to the large cross talking observed within the SCSI cables, other alternatives such as the coaxial cable need to be explored.

Coaxial Cables

The coaxial cables have been proposed as the cable for the new TIG64 data acquisition system along with the SCSI connections to terminate the data transfer. The SCSI connectors have been tested for cross talk (see Cross Talk with SCSI Connectors) and resulted in a 0.5% cross talk on a 1.0V input signal. The coaxial cables must now be tested to complete the cross talk tests for the proposed system. As seen in Figure 3.2.3, the 50 foot coaxial cable is not terminated by SCSI connections. This is to ensure that all of the cross talk comes from the cable itself. The channel set up was different compared to the SCSI connections. There were only 16 channels within these cables. To test the cross talking, channels 1, 4, 8, 12 and 16 were used as input channels. Throughout all of the tests, channel 14 did not give any cross talk however this is potentially due to a faulty connection in one of the connectors at either end of the coaxial cable.



Figure 3.2.3. Coaxial cable used to test cross talking for the new data acquisition system.

The images within Appendix II indicate cross talking trials from within a coaxial cable. The coaxial cables were terminated using a connection that converted the signal into limo cables as seen in Figure 3. As mentioned before, channel 14 appears to have no cross talking throughout these images however it is likely due to a faulty connection. Note the scales of both the voltage and time throughout all of the images. The cross talk channels have a voltage scale of 5mV and a time scale of 100 μ s. The cross talking signals appear to have an average peak to peak voltage of around 10mV while the signals last for the length of the square wave. These signals indicate a 1% cross talk affect from the 1.0 V input signal. A 10mV signal is not large enough to cause a false trigger from the TIGRESS array. Therefore, the coaxial cables are an acceptable solution to the current cross talk being observed within the SCSI cables.

3.3 – TBragg Simulations

The TRIUMF Bragg detector lies on the beam line SEBT3 just north of TIGRESS. It is a diagnostic, ionization chamber used to determine beam composition. An ionization chamber is filled with gas and isotopes entering the chamber lose energy as they interact with the gas within the chamber. The isotopes will interact with electrons, exciting them and causing the electrons to leave their atom, ionizing the gas. The entire length of the chamber is lined with electrode rings used to accelerate the free electrons towards an anode at the end of the chamber where they are collected. The charge collected is proportional to the energy lost as the isotopes move through the chamber. The chamber itself is approximately 10cm in length (according to specifications) with a $1.5\mu\text{m}$ mylar window at the beginning of the chamber and a Frisch grid directly before the anode.

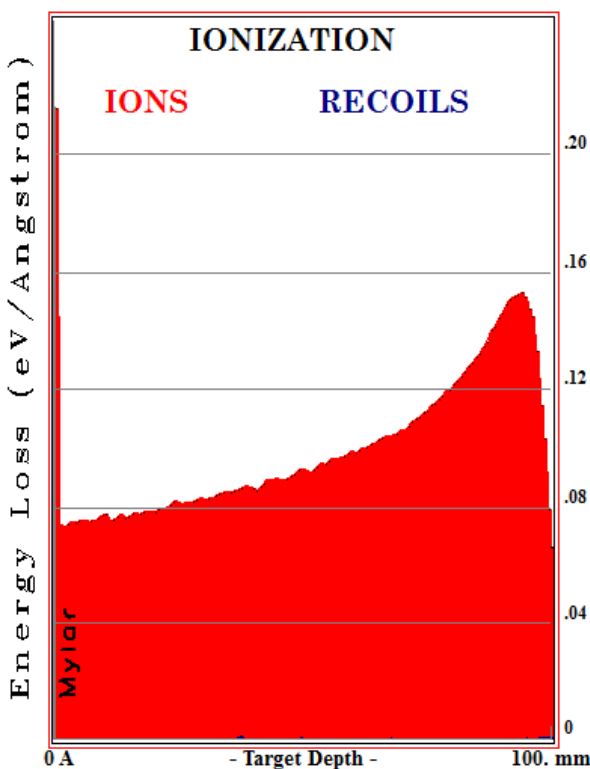


Figure 3.3.1.Bragg curve created by the SRIM software for ${}^{20}\text{Ne}$ at 99MeV. The peak is apparent and has a high Z dependence which is useful in particle identification.

Once the charge has been collected on the anode, the total charge collected is sent to a pre-amplifier. These pre-amplifiers then apply both short and long energy filters to the anode signal. The short and long filters create two windows with varying size (depending on the filter) and the values inside these windows are averaged. The averaged values from each window are then subtracted giving a value for that filter. The windows are then stepped across the entire range repeating this process. Finally, the maximum value of this difference is stored as the value from that filter. A short filter has a much smaller window as well as a smaller gap between the windows and thus measures the peak of a Bragg curve (Figure 1) which has a high Z dependence. Meanwhile, the long filter has a longer window and gap and thus it effectively measures the total energy deposited within the chamber. The values are then plotted on a histogram of short filter, long filter and counts (Figure 2).

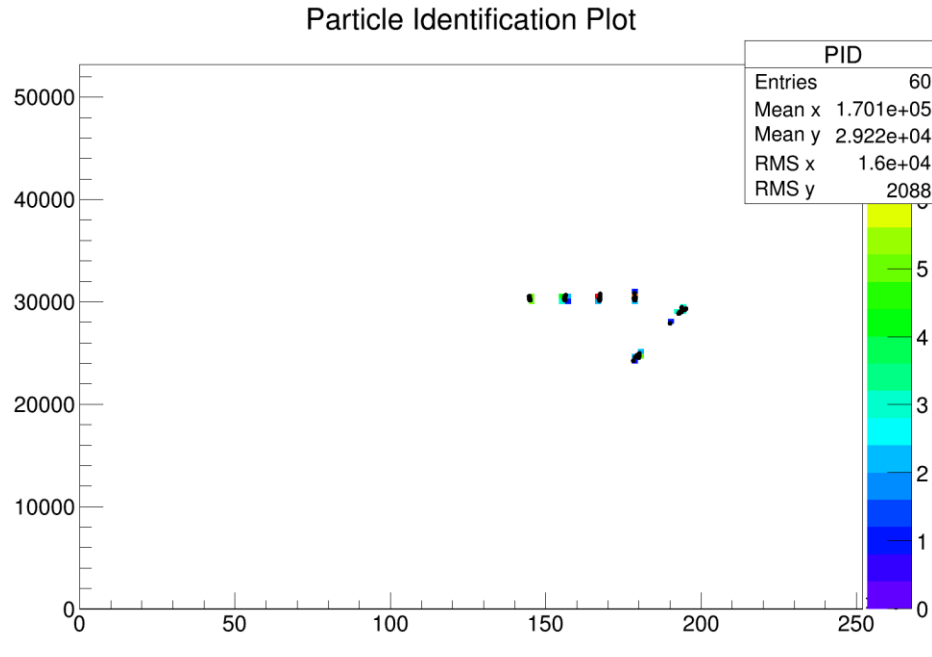


Figure 3.3.2. A sample particle identification plot from simulation with the short filter value plotted on the y axis and the long filter value on the x axis. This is a series of energies from 6.05MeV/u to 8.00 MeV/u for ^{28}Si at 950 torr (ie., 0.001944g/cm³ in SRIM simulation).

Simulations were needed to help determine the locations of isotopes relative to each other. The SRIM software was used to create collision files of isotopes entering the TBragg. These files contained the information (including energy remaining and position) about collisions that occur within the chamber. To create these files, enter the SRIM software and open the window called TRIM. This will open a window allowing the element, energy and mass of the isotope to be set as well as the type of material within the chamber. The material that the isotope passes through is first a 1.5 μm mylar window before passing through a working volume of 10cm. This volume is filled with gas, usually P-8 gas. P-8 gas is 92 parts argon and 8 parts methane leaving the ratio of 92:8:32 (Ar : C : H). Using molar masses and the ideal gas law, the density can be varied to account for different pressures. At a pressure of 760 torr, the density should be 0.001544g/cm³. Once all of these values are set, the simulation can be run. It only needs to be run for around 10 ions but this can be set to any value. Once the simulation is complete, the collision file required with the C++ code can be found under SRIM outputs in the directory to which SRIM was downloaded. The other figure of interest can be found on the main simulation screen. Selecting "Ionization" will bring up the Bragg curve that can be seen in Figure 3.3.1.

In conjunction with the SRIM simulations, several versions of a C++ code were written to simulate the anode and pre-amp response. This code receives the collision files from SRIM and analyzes the data to create long and short filter values for each ion. The original code written by

Tanner Bruhn was ineffective and was needlessly complicated due to the nested vectors. The simulations appeared to hold true until ions began to pass through the chamber without losing all of their energy (punch through). This punch through occurred when using the simulations for the 2015 SHARC experiment S1554 with ^{28}Si at energies of around 8.00MeV/u. This error occurred as the limits were not properly taken into account. For example, the final energy was defined as zero which caused a mismatch in the averaging, creating a larger value for both the short and long integration times. Figure 1 indicates the proper appearance of the long and short filters with proper boundary conditions of the new code.

A new code was written this summer and it has better results than the previous code. It was written in C++ as well however it used single arrays instead of nested vectors making it simpler. This code takes into account the boundary conditions so isotopes punching through are properly analyzed as seen in Figure 3.3.2. The code begins by creating a series of times that correspond to the total number of samples (dependent on drift velocity and chamber length) and the analog-to-digital converter sample rate. These times are the points at which a sample will be taken from the anode. These times are then converted to corresponding distances within the chamber. The collision text files produced by the SRIM program are then read into the C++ program. The program reads through each line to find a distance that is closest to the simulated distance and subsequently reads the corresponding energy. This creates both a position and energy arrays that can be put through energy filters. Short and long energy filters are applied and the values from each ion are printed to the screen along with the initial conditions of the isotope. Using a simple histogram program, these can then be piped into a histogram plot.

Table 3.3.1. Parameters as seen in the most recent code, TBraggSimulation_v5.cpp. Each parameter can be changed in the command line.

Parameter	Standard Value
adcSampleRate	0.02 μs
l_peakt	0.5 μs
l_gapt	4.5 μs
s_peakt	0.14 μs
s_gapt	0.24 μs
driftVel	4.8 cm/ μs
minDepth	15000 A
maxDepth	10.00 cm

There are several parameters that change the effects of the filters as well as the number of samples. Table 3.3.1 indicates the standard values for each of parameters as determined by the manufacturers of the TBragg. The adcSampleRate is the rate at which the analog-to-digital converter (adc) samples the anode signal. This will affect the number of samples taken for any given ion. The peakt indicates the peak time within a given window. Dividing the peak time by the sample rate gives the number of samples within the given window. Similarly, the gap time (gapt) is the time between windows. This can also be turned into number of samples. The drift velocity (driftVel) is dependent on the strength of the electric field applied by the electrodes. At a high voltage bias of 1560V and a pressure of 900 torr, the drift velocity is 4.8 cm/ μ s. Keeping the ratio of voltage and pressure constant will allow for a constant drift velocity. The minimum and maximum depths correspond to the beginning and end of the gas. Therefore minDepth corresponds, in this case, to the width of the mylar window and maxDepth corresponds to the length of the chamber. All of these parameters can be changed within the command line while calling the program by adding a “- -” before the value. For example, the command line “./TBraggSimulation --l_peakt 0.4 Si28.txt” would change the long peak time to 0.4 μ s before analyzing the Si28.txt collision file.

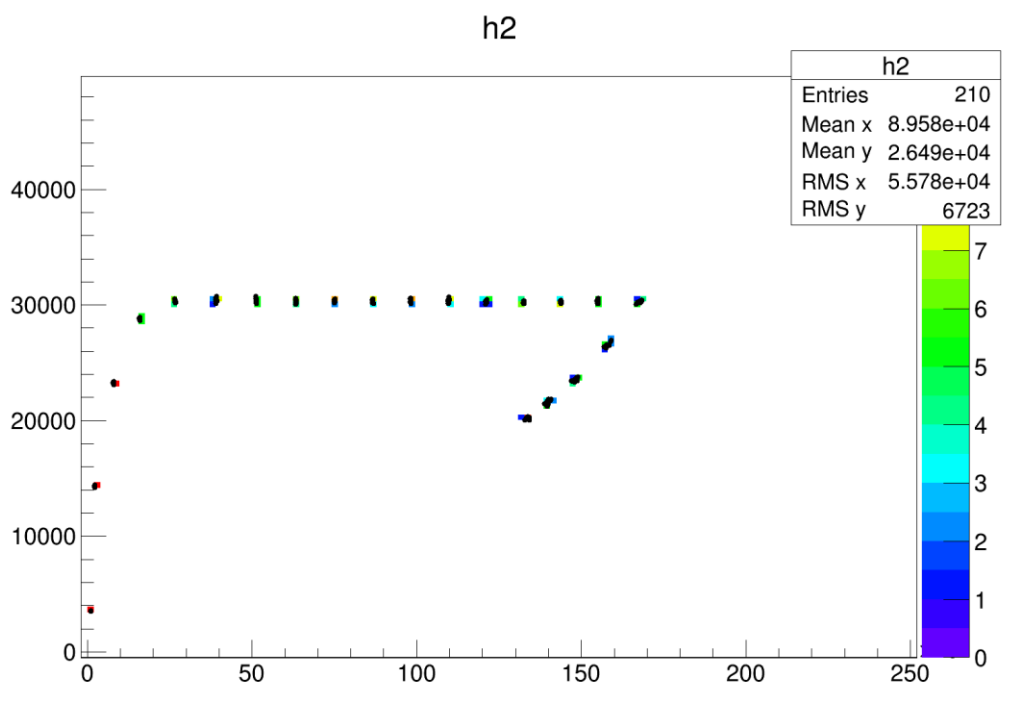


Figure 3.3.3. Spectrum of ^{28}Si with a working chamber length of 10.00cm. The energy series runs from 8.00MeV/u to 0.00MeV/u in a pressure of 950torr. The short values are displayed on the y-axis and the long values displayed on the x-axis.

During the 2015 SHARC experiment S1554, there were many issues with beam contaminants as well as punch through of the TBragg due to the high energy nature of the experiment. TBragg spectra of ^{28}Si and ^{12}C indicated large curves such as Figure 2 due to large punch through. However when these spectra were simulated with the newest code, the spectra did not appear the same. Figure 3.3.2 indicates a working chamber length of 12.28cm while Figure 3.3.3 indicates a working chamber length of 10.00cm. Note that there is a shift in the long filter that causes a slight increase as well as a shorter tail before the turn. Figure 4 indicates the data taken by the TBragg (TBragg Elog entry 210) and matches more closely to the value of Figure 3.3.2. The same effect was observed in spectrums of ^{12}C (TBragg Elog entry 209). This indicates that the working chamber length of the TBragg is longer than expected or perhaps there is some dead volume near the beginning of the chamber. Both of these need to be explored in greater detail, either through further simulations and data calibration or by looking at the TBragg itself.

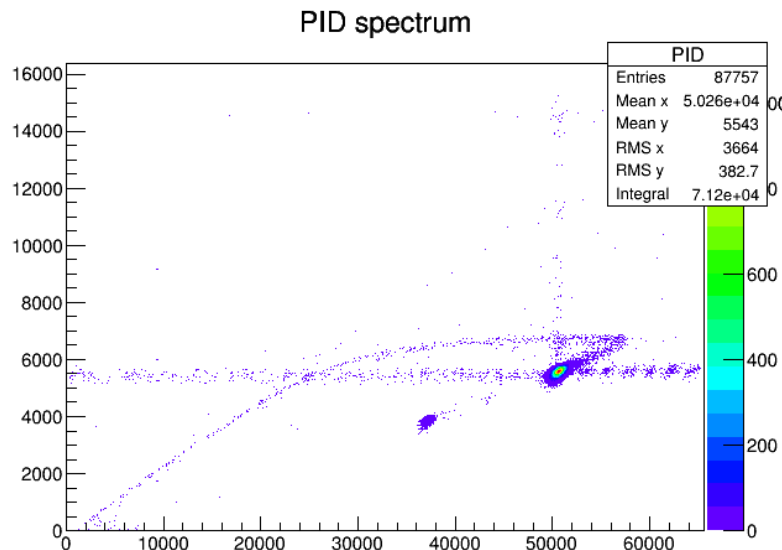


Figure 3.3.4. Data taken using the TBragg during the S1554 SHARC experiment. The large spot indicates ^{28}Si within the beam. This image compares well to Figure 2 due to the length of the tail.

The TBragg device in conjunction with simulations still requires investigation as there are several aspects that could be improved. The simulations (including C++ code) have improved but could also be added to including a pre-amp response time that causes a rounder signal compared to the current signal. There are several other factors that should be taken into account to improve the simulations and thus there is definitely room for improvement. However, the simulations have also brought up questions about the TBragg chamber itself including the working chamber length and possible dead space at the front of the chamber. These two aspects should be explored further with simulations and data calibrations.

5 – Conclusion

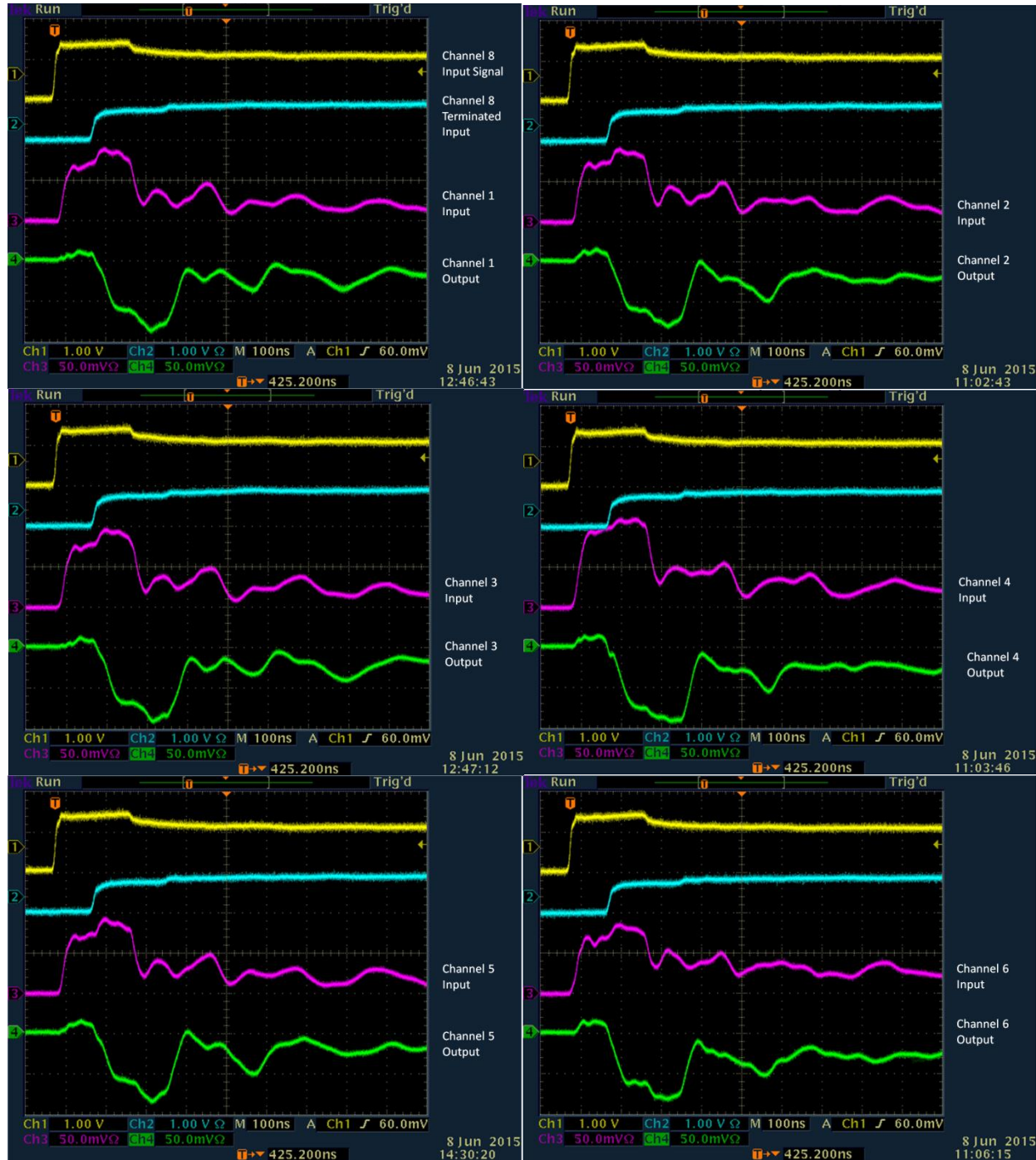
Gamma ray spectroscopy consists of three main components apart from experimentation itself: data acquisition, detectors and beam identification. Throughout the work term with TRIUMF, the projects and scientific experimentation covered all of these topics. The SCSI cross talk testing was aimed to aid in the development of a new DAQ, while the CAEN MCA will be used for detector testing and finally the TBragg detector and simulations will be used together to help with beam identification. The projects have given me insight into the world of gamma ray spectroscopy as well as the world of research.

References

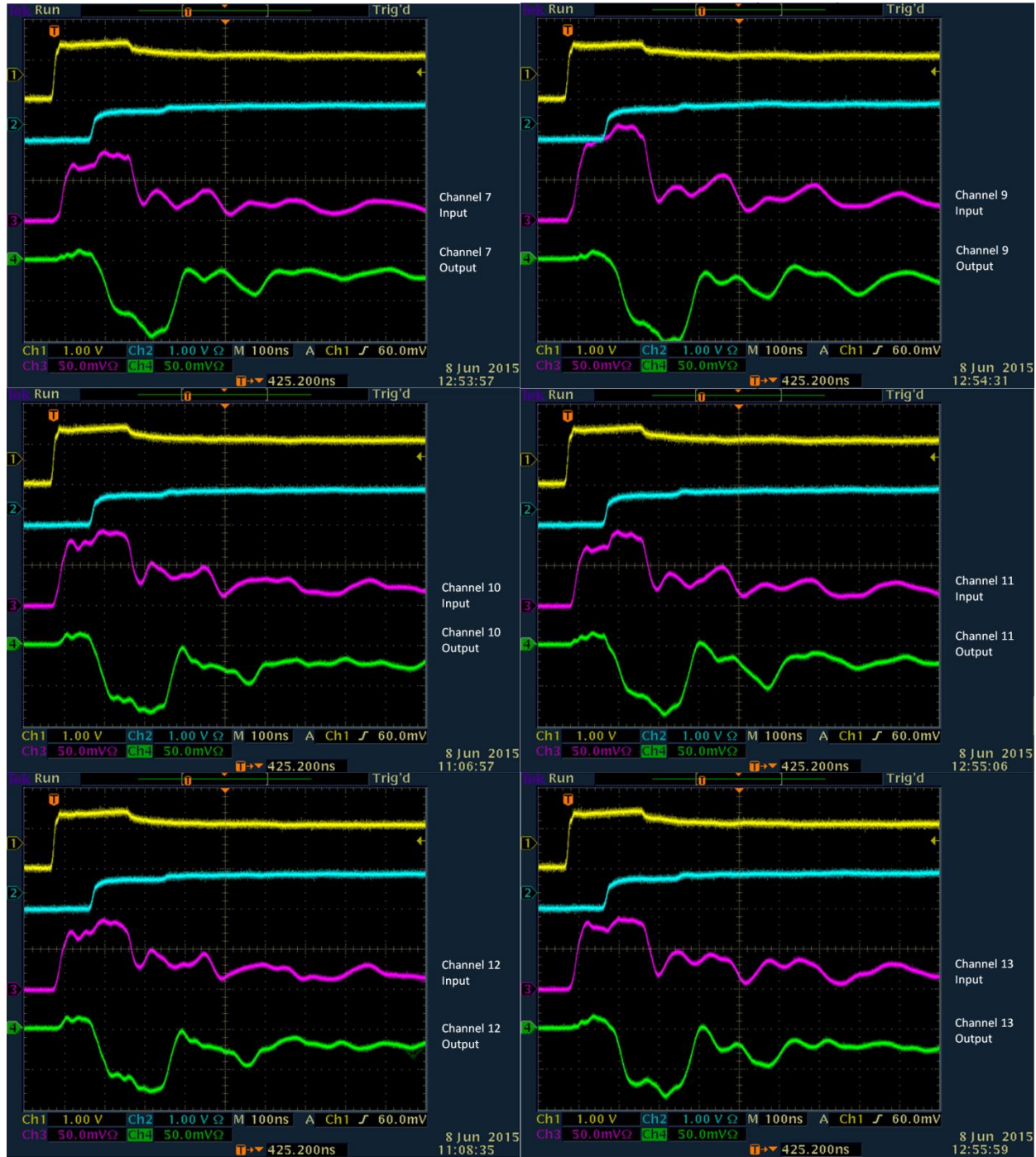
- [1] CAEN, "CAEN Electronic Instrumentation," 26 January 2015. [Online]. Available:
] <http://www.caen.it/jsp/Template2/LibrarySearchResults.jsp?browse=n&keywords=MC2&type=Manuals>. [Accessed 19 May 2015].
- [2] R. Dunlap, An Introduction to the Physics of Nuclei and Particles, Belmont: Brooks, 2004.
]
- [3] S. Tavernier, Experimental Techniques in Nuclear and Particle Physics, Brussels: Pringer-Verlag Berlin
] Heidelberg, 2010.

Appendix I - SCSI Connections and Cable Cross Talk Images

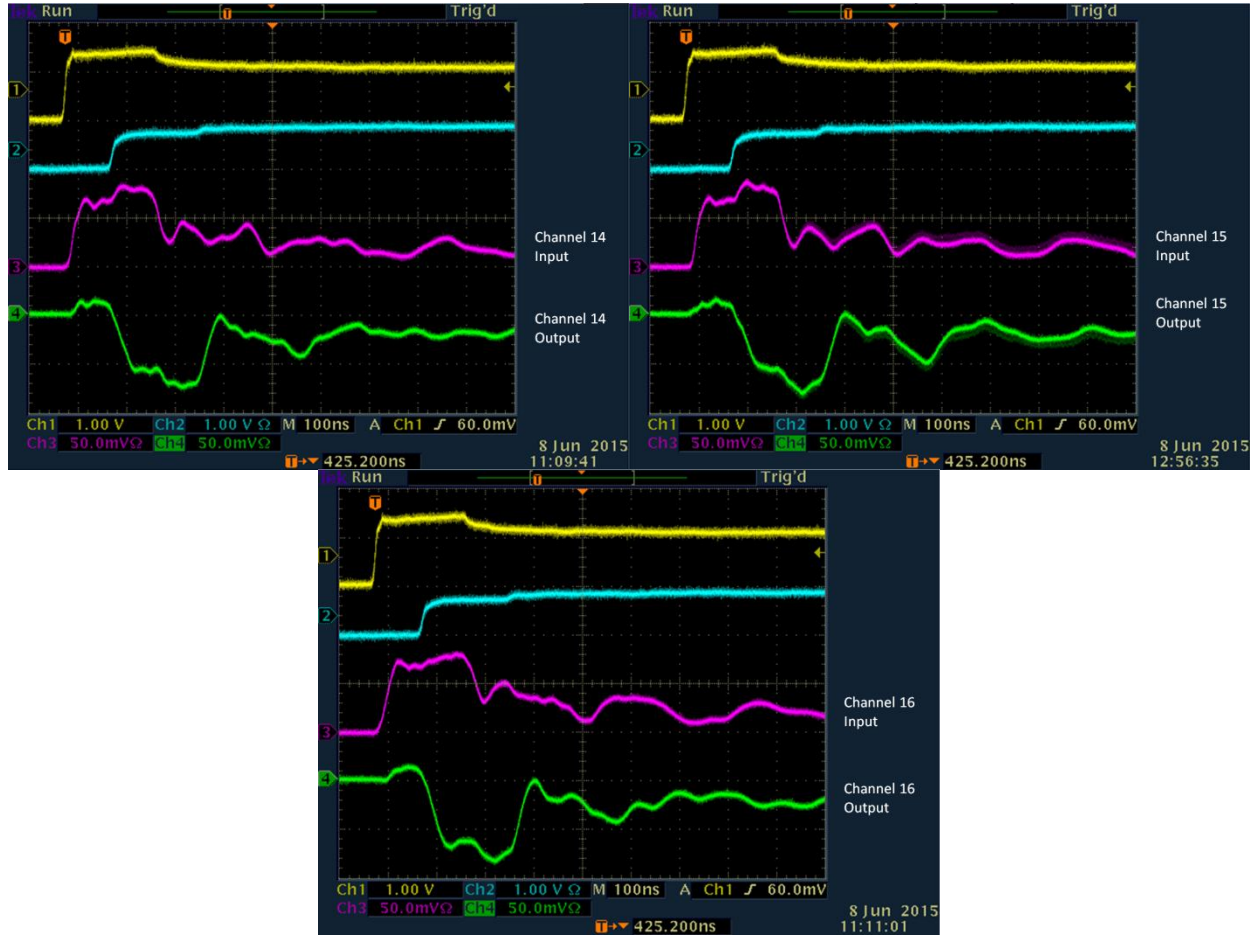
Channel 8 Cross Talk Images



Appendix I - SCSI Connections and Cable Cross Talk Images

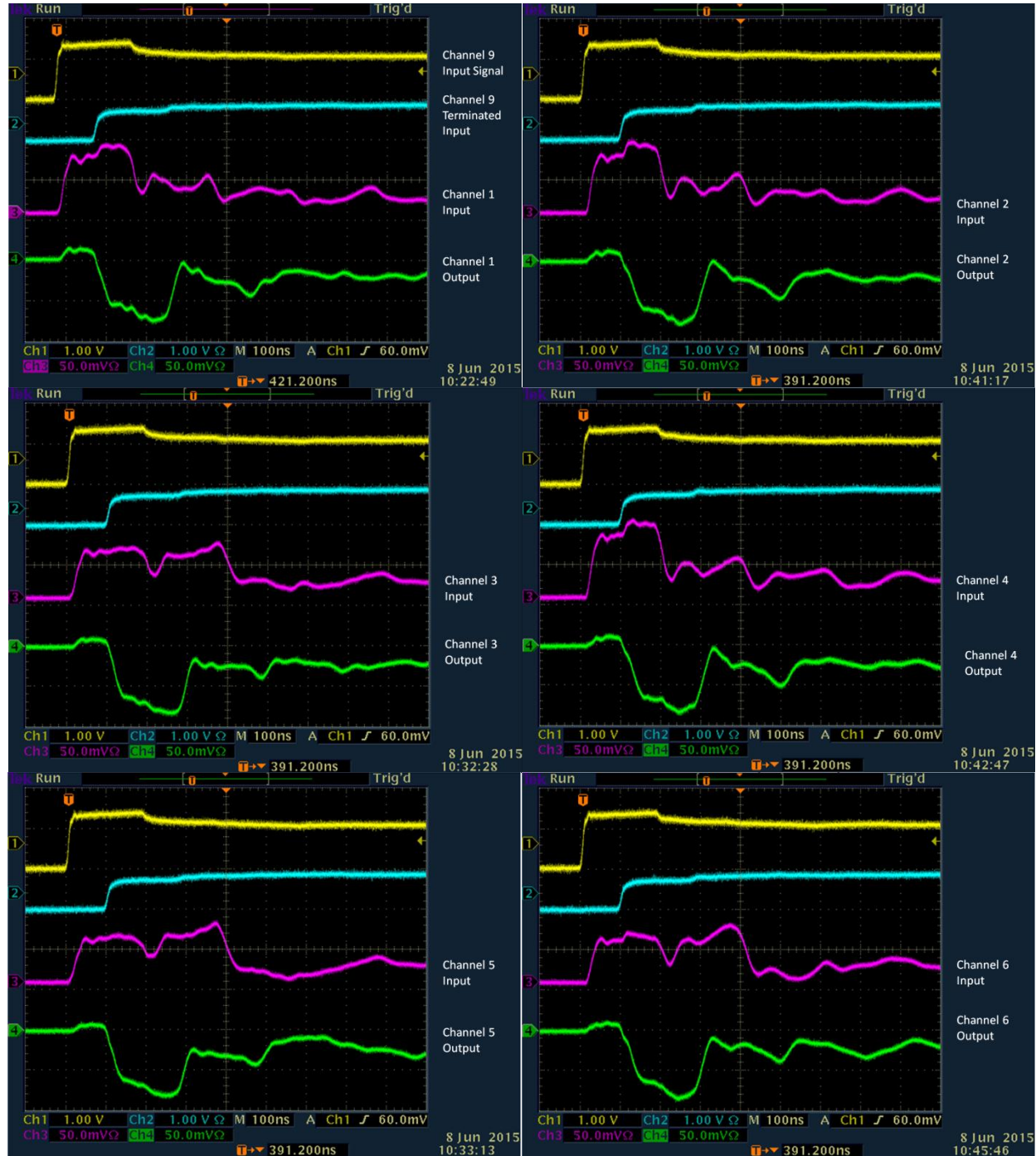


Appendix I - SCSI Connections and Cable Cross Talk Images

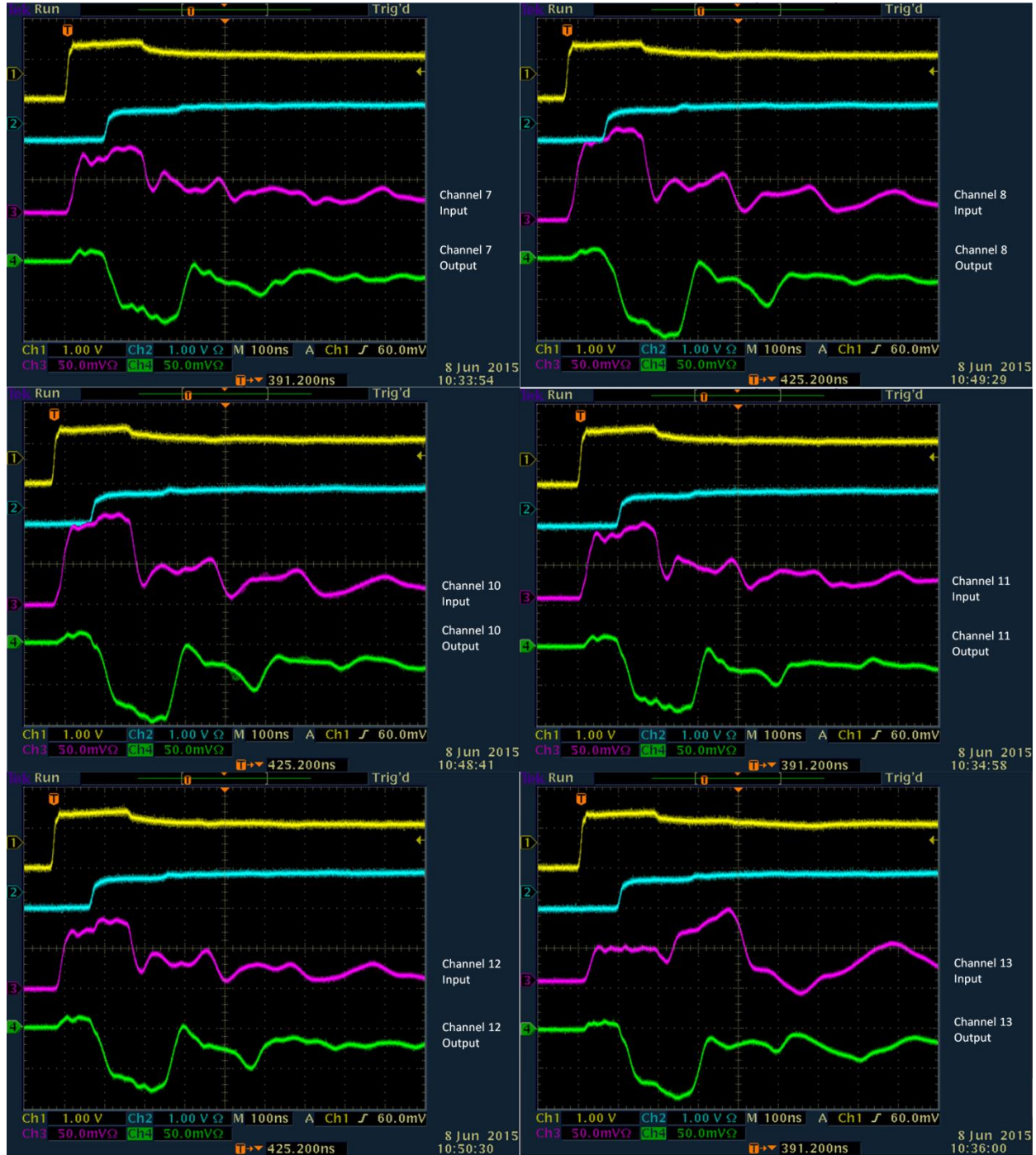


Appendix I - SCSI Connections and Cable Cross Talk Images

Channel 9 Cross Talk Images



Appendix I - SCSI Connections and Cable Cross Talk Images

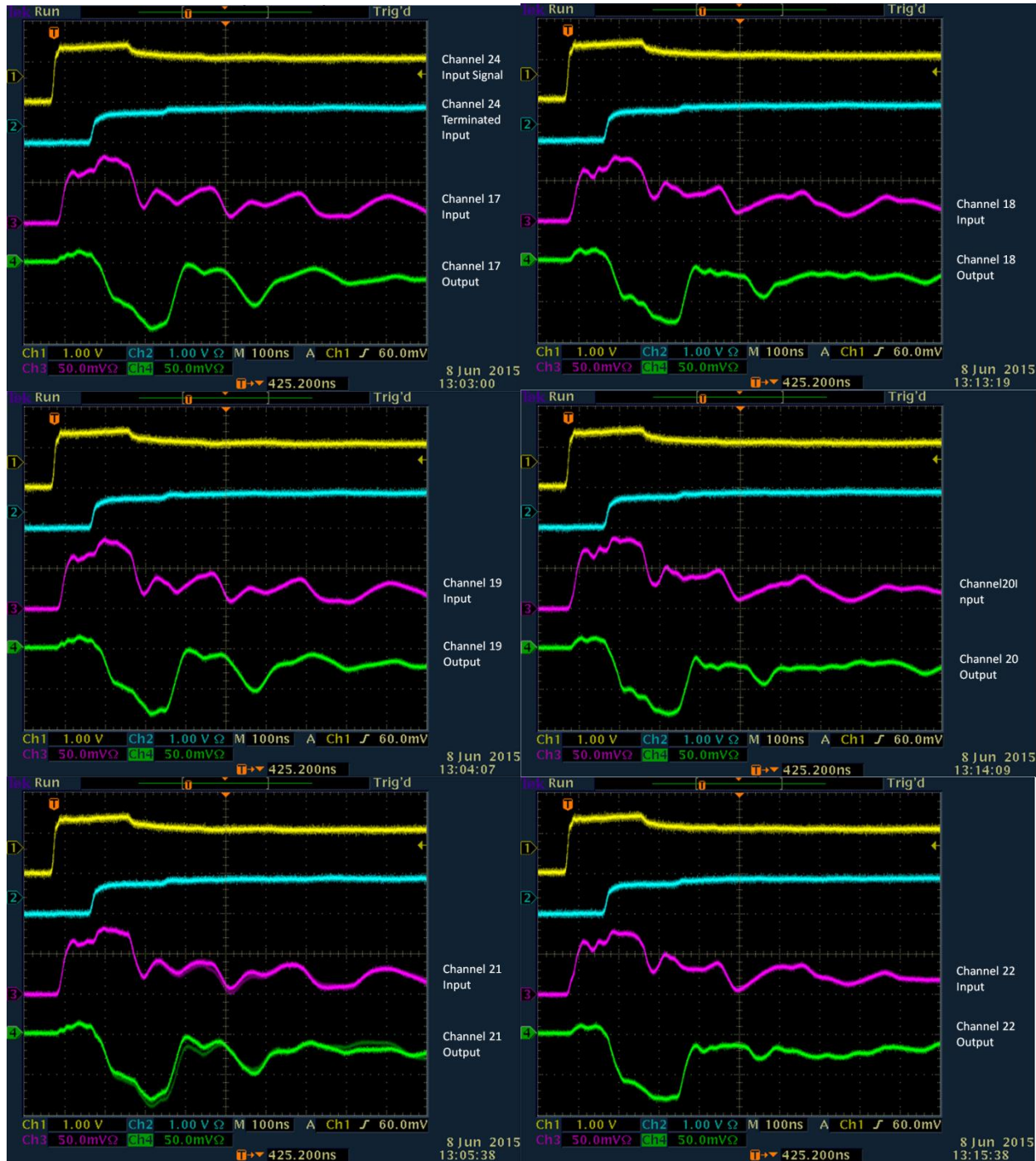


Appendix I - SCSI Connections and Cable Cross Talk Images

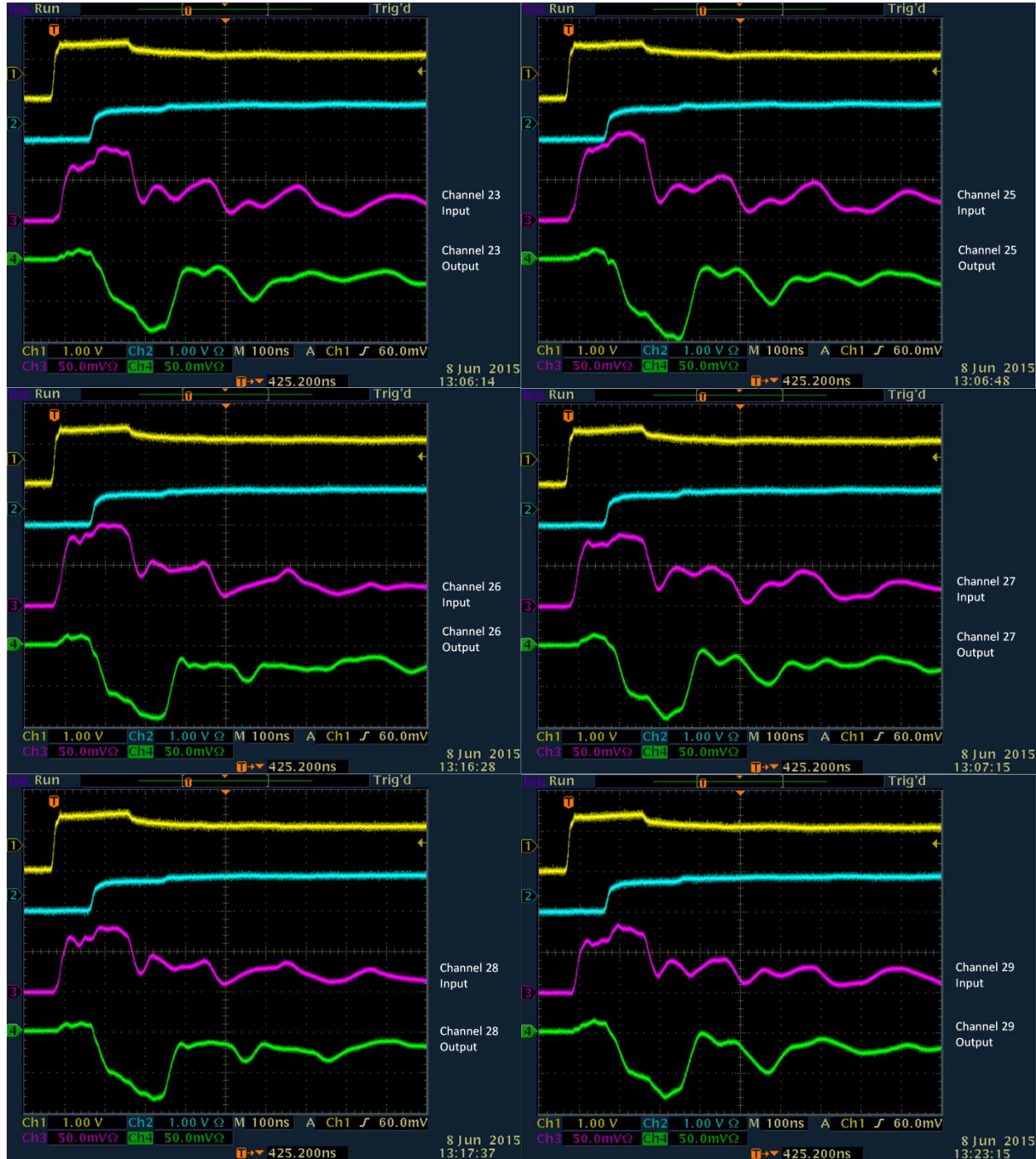


Appendix I - SCSI Connections and Cable Cross Talk Images

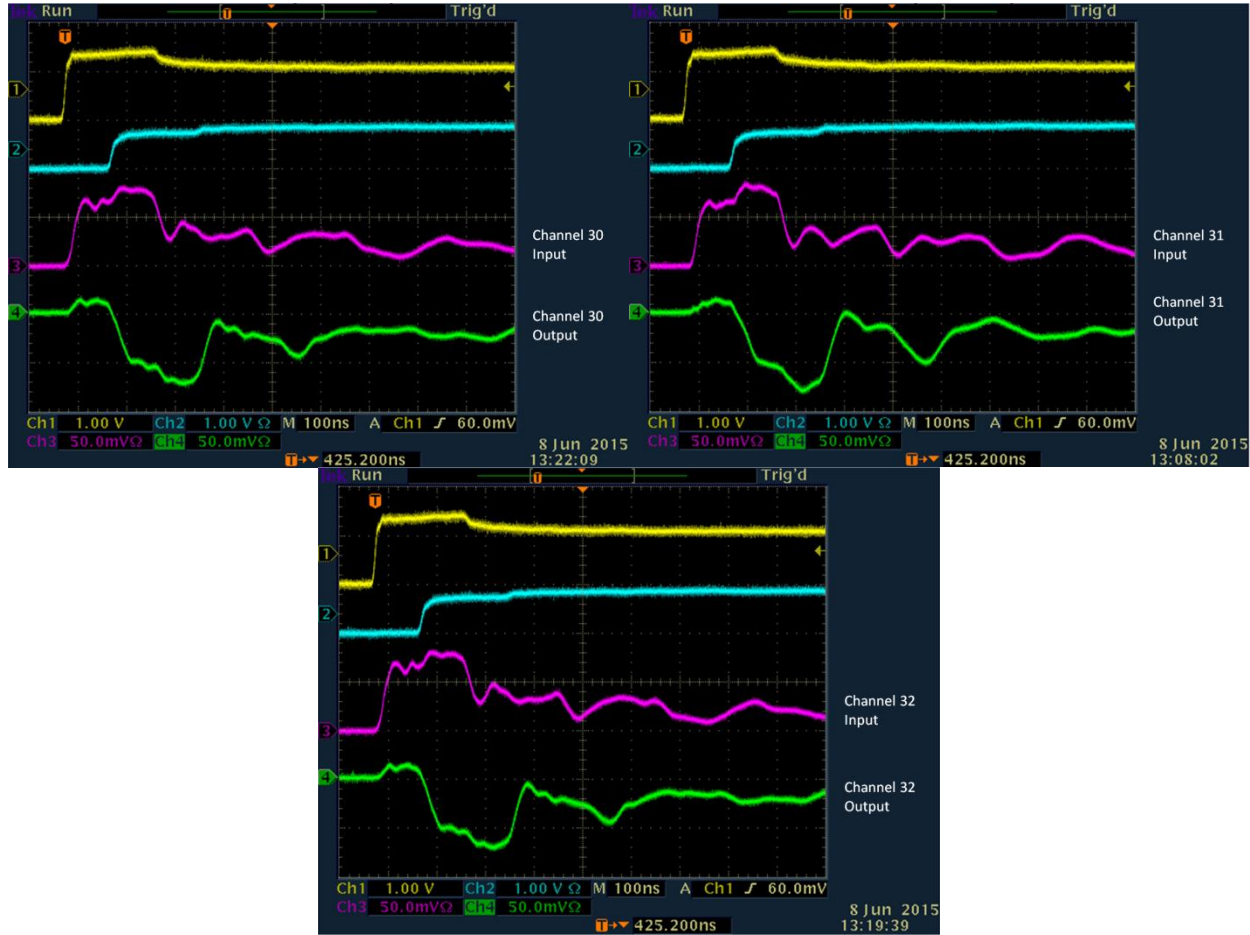
Channel 24 Cross Talk Images



Appendix I - SCSI Connections and Cable Cross Talk Images

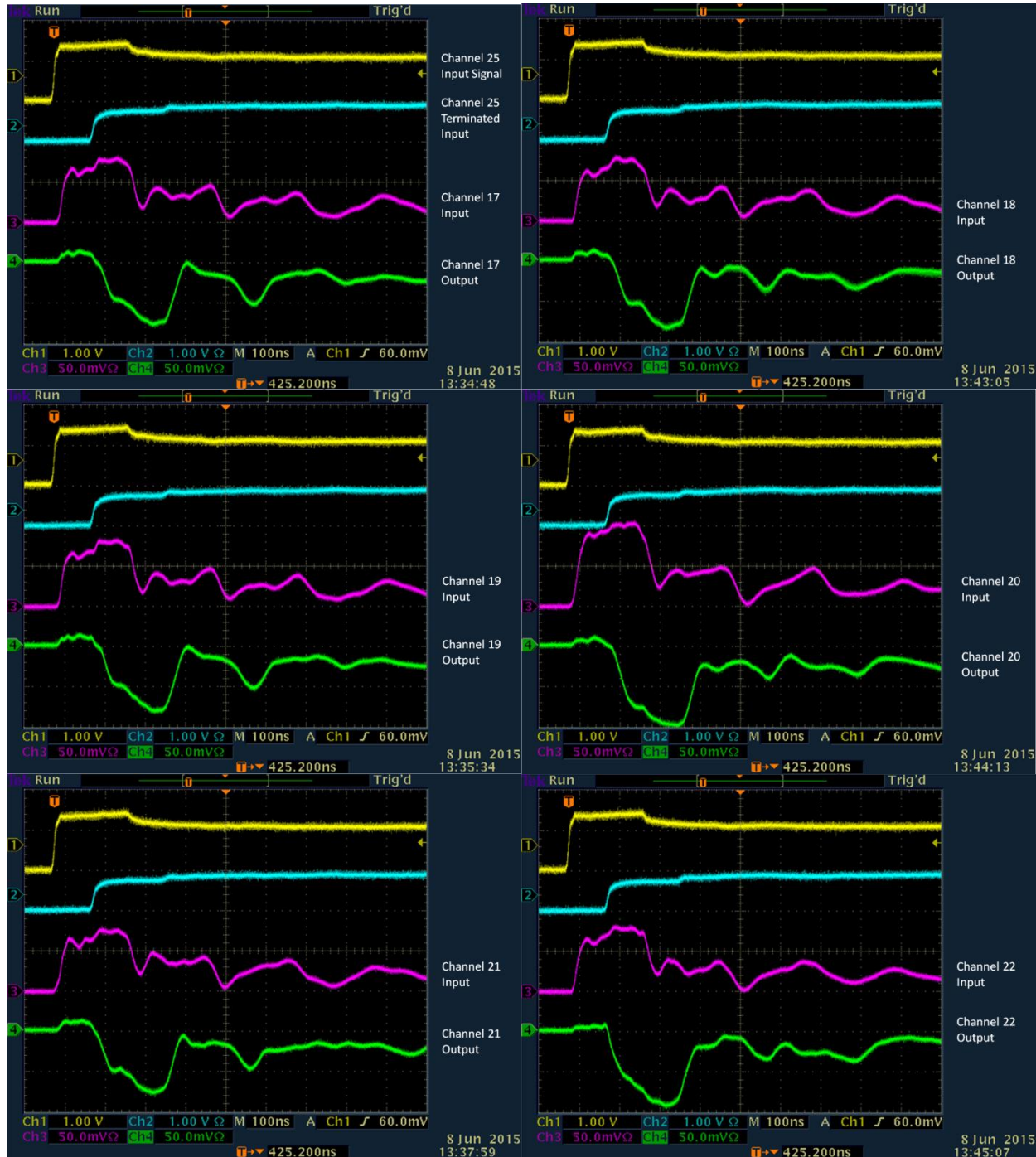


Appendix I - SCSI Connections and Cable Cross Talk Images

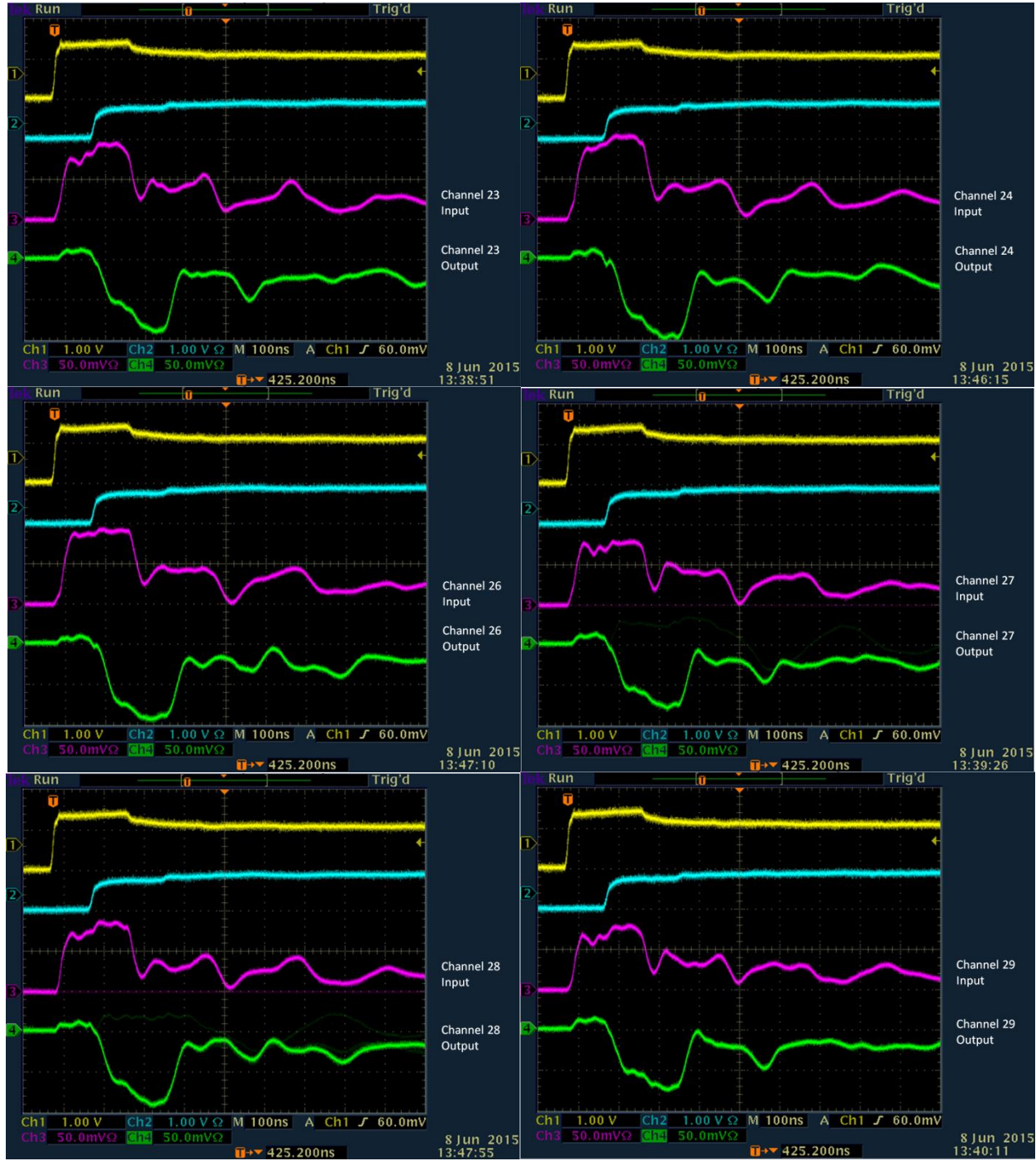


Appendix I - SCSI Connections and Cable Cross Talk Images

Channel 24 Cross Talk Images



Appendix I - SCSI Connections and Cable Cross Talk Images

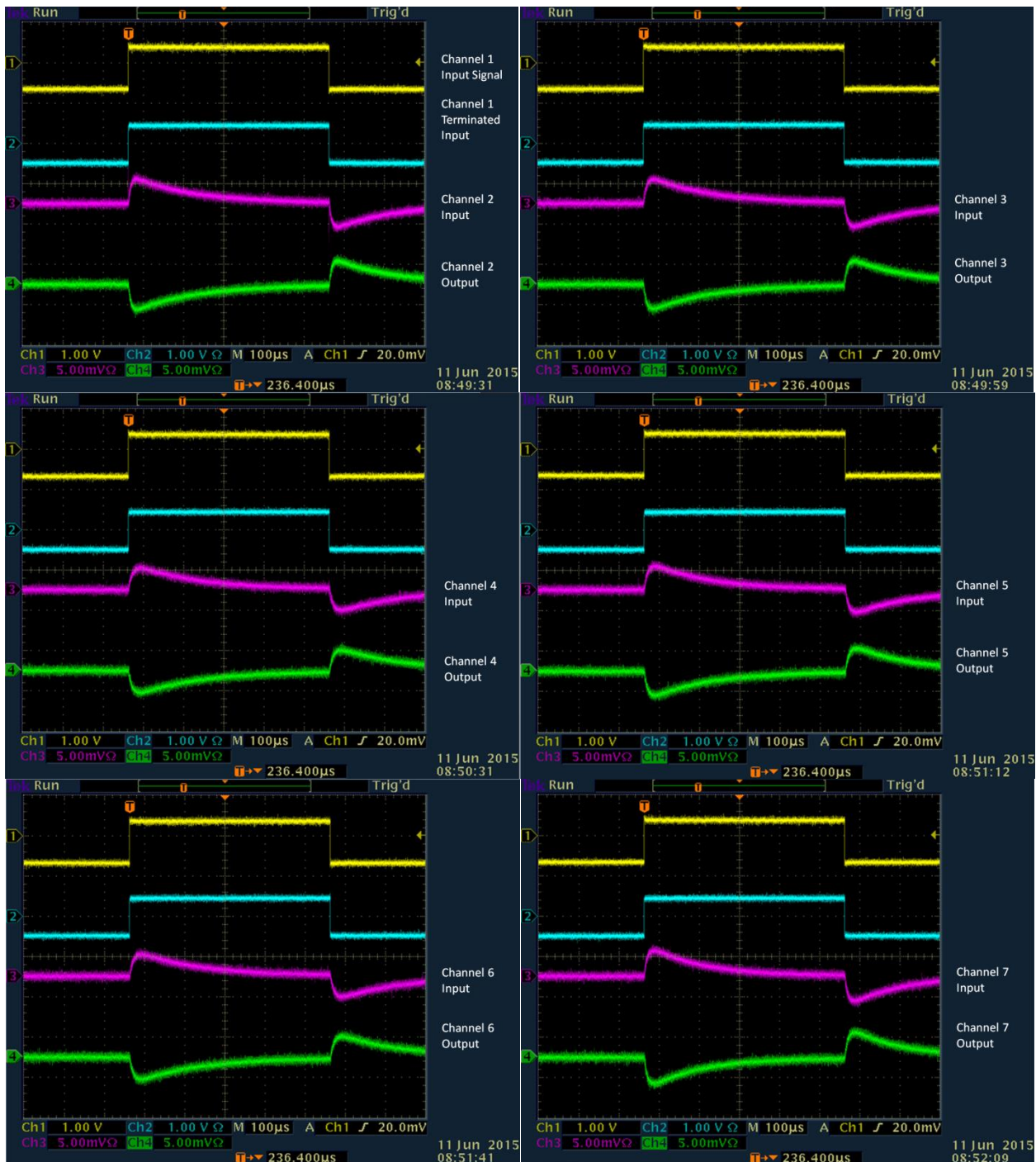


Appendix I - SCSI Connections and Cable Cross Talk Images

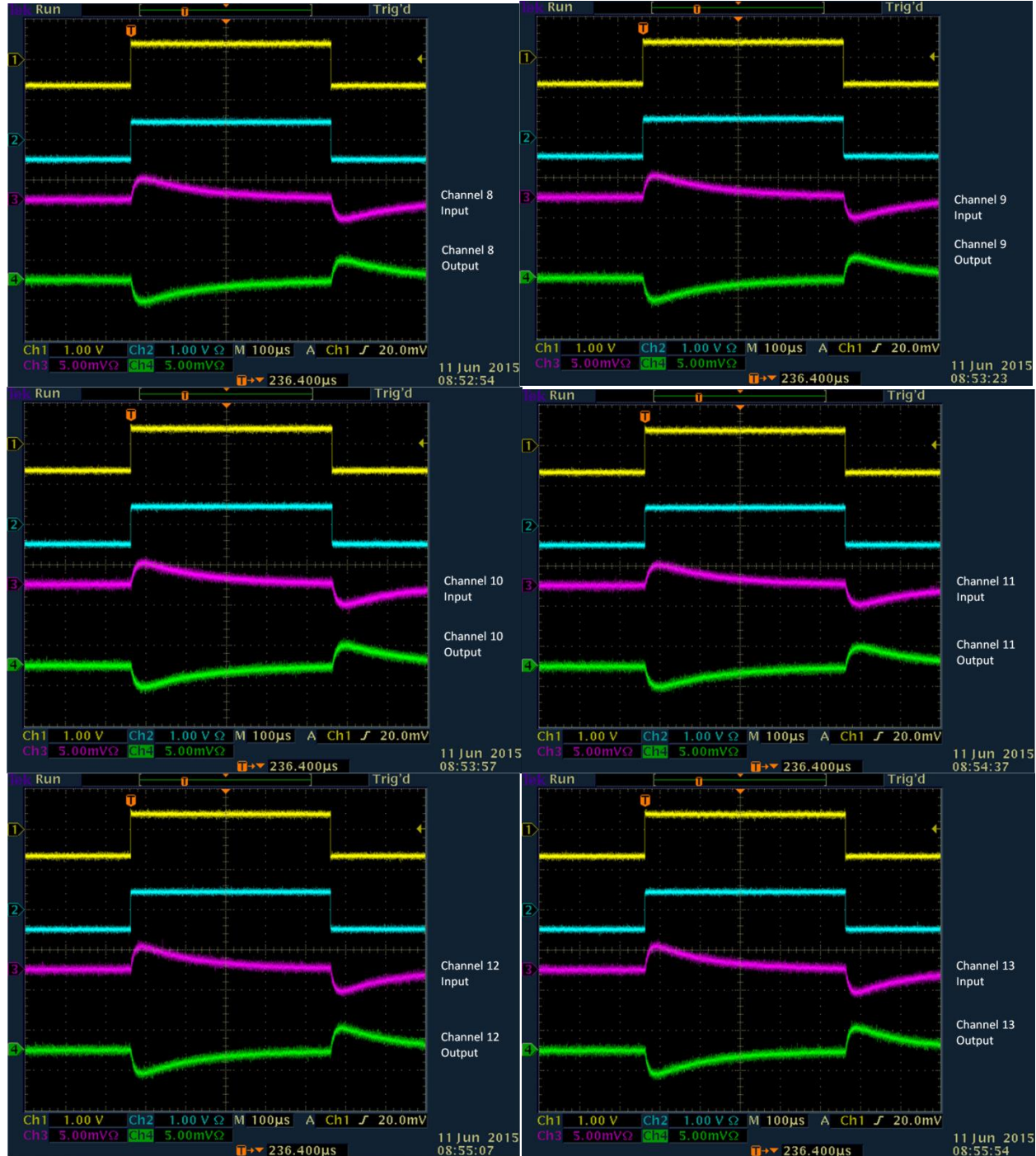


Appendix II - Coaxial Cables Cross Talk Images

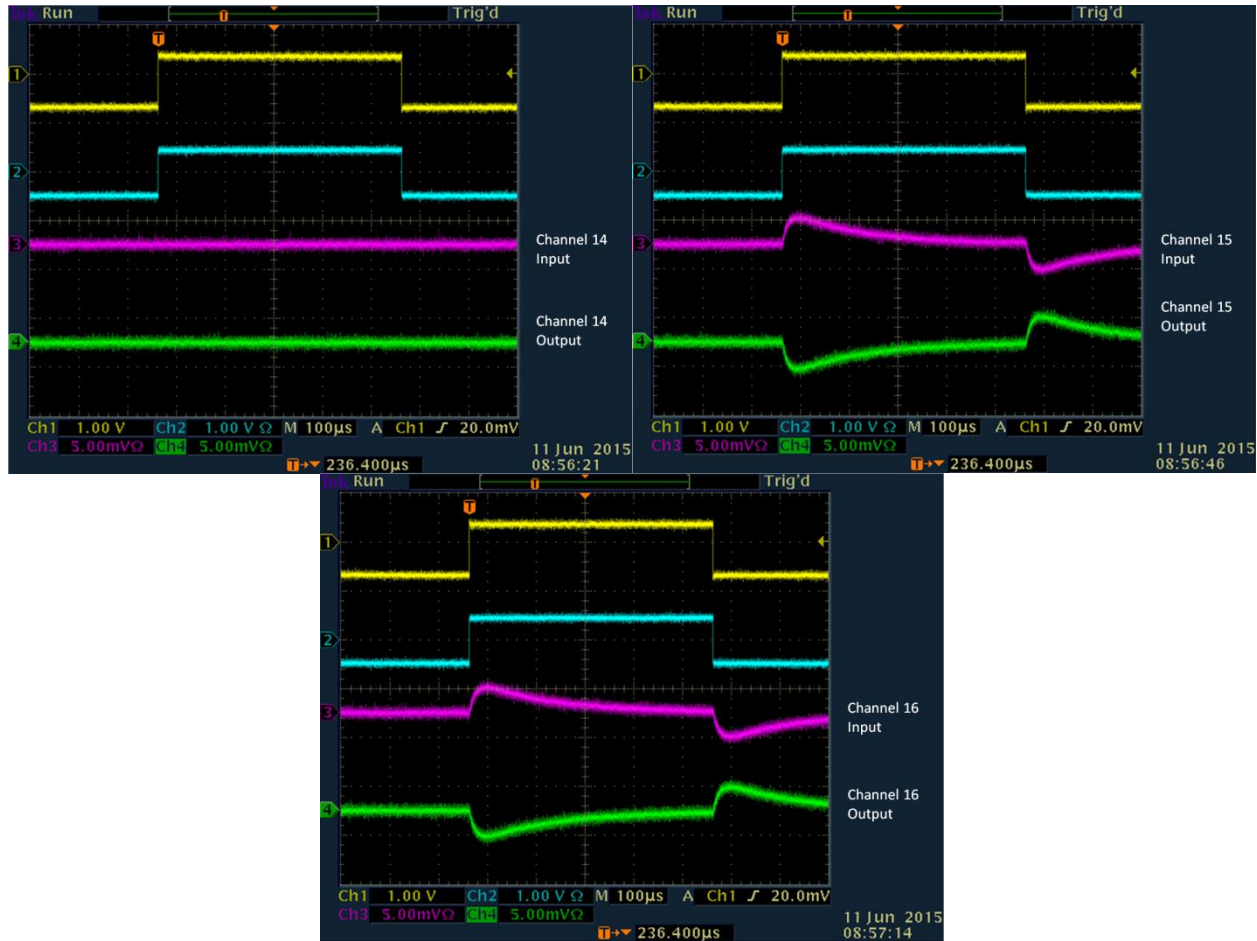
Channel 1 Cross Talk Images



Appendix II - Coaxial Cables Cross Talk Images

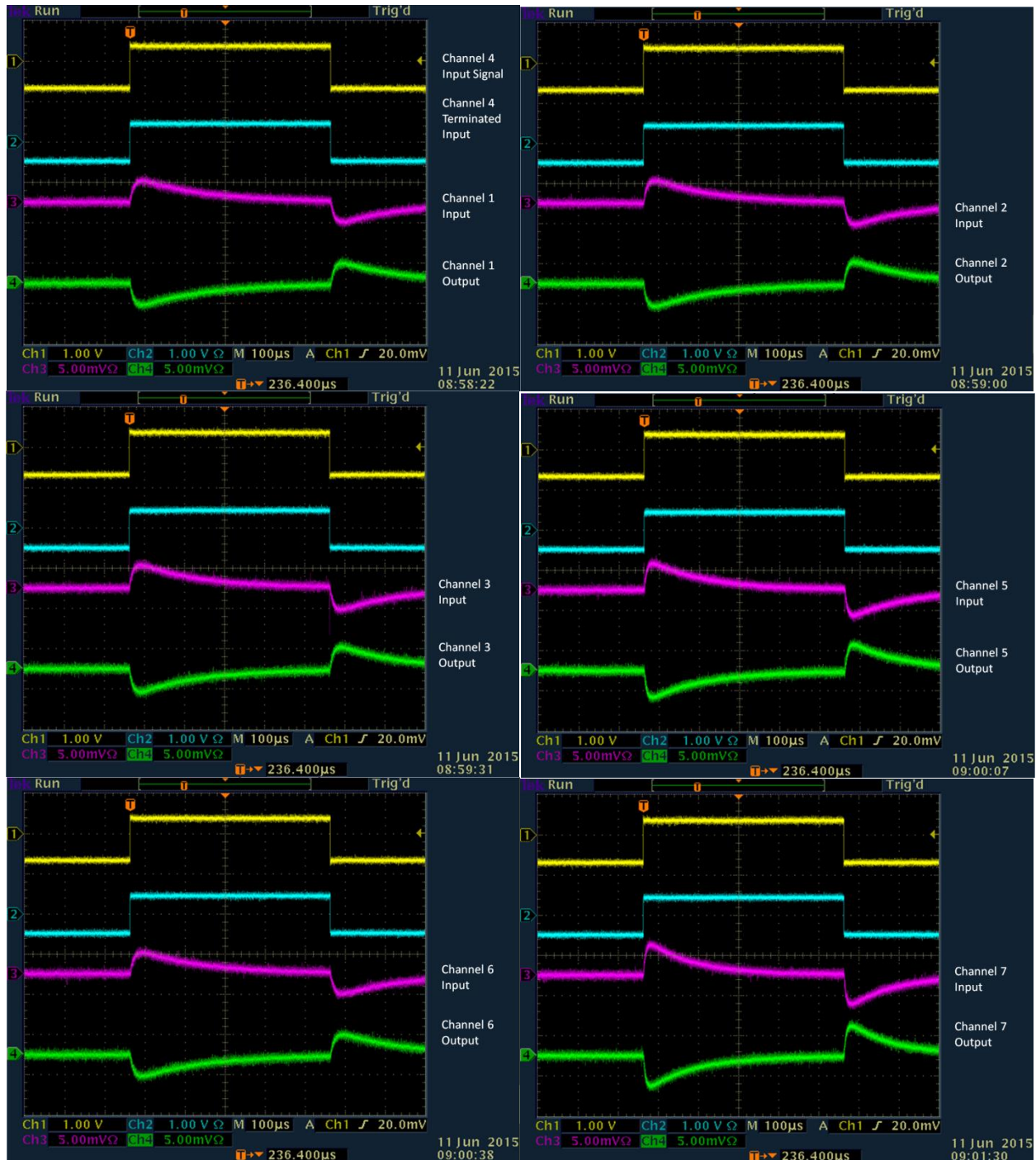


Appendix II - Coaxial Cables Cross Talk Images

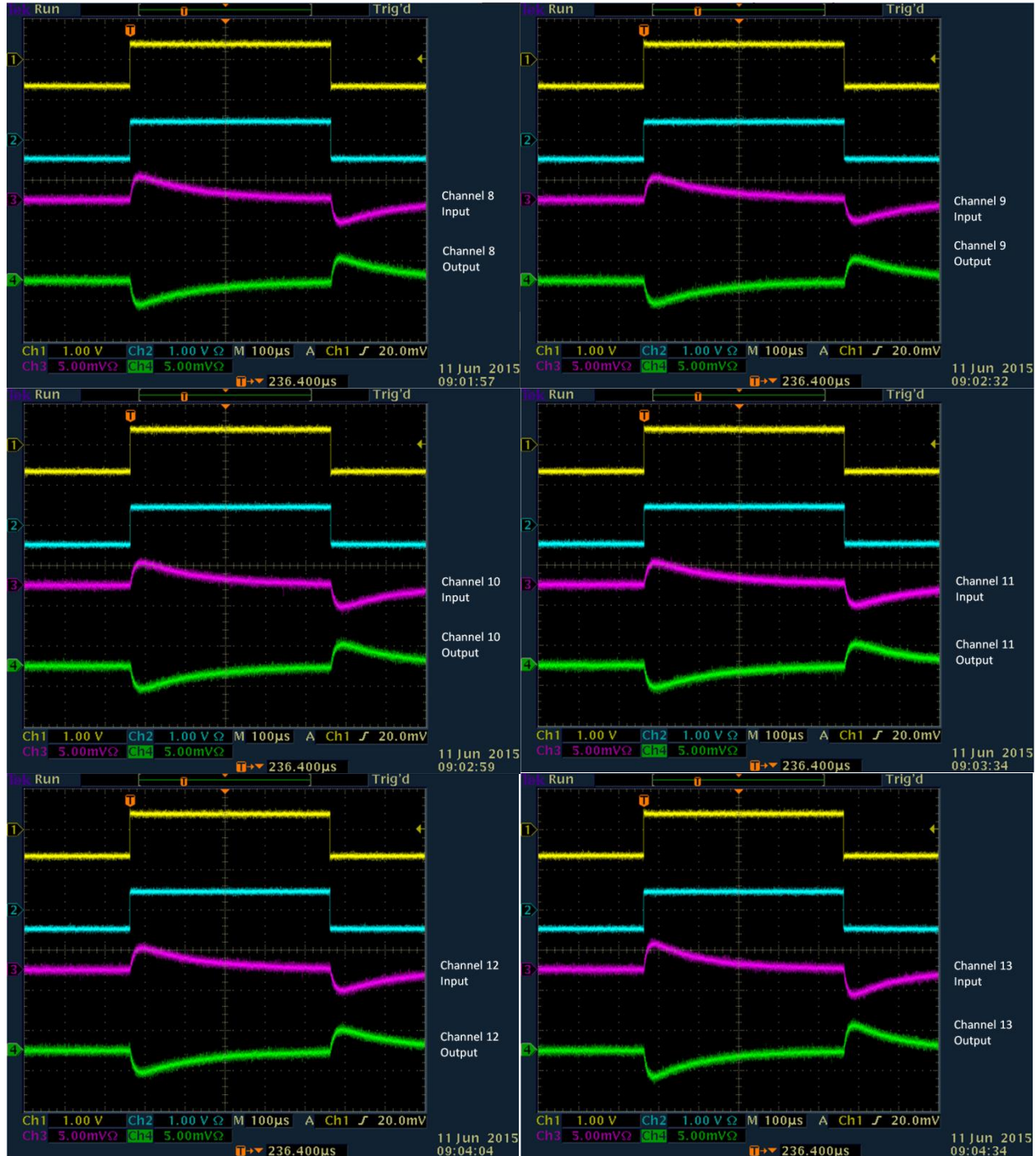


Appendix II - Coaxial Cables Cross Talk Images

Channel 4 Cross Talk Images



Appendix II - Coaxial Cables Cross Talk Images

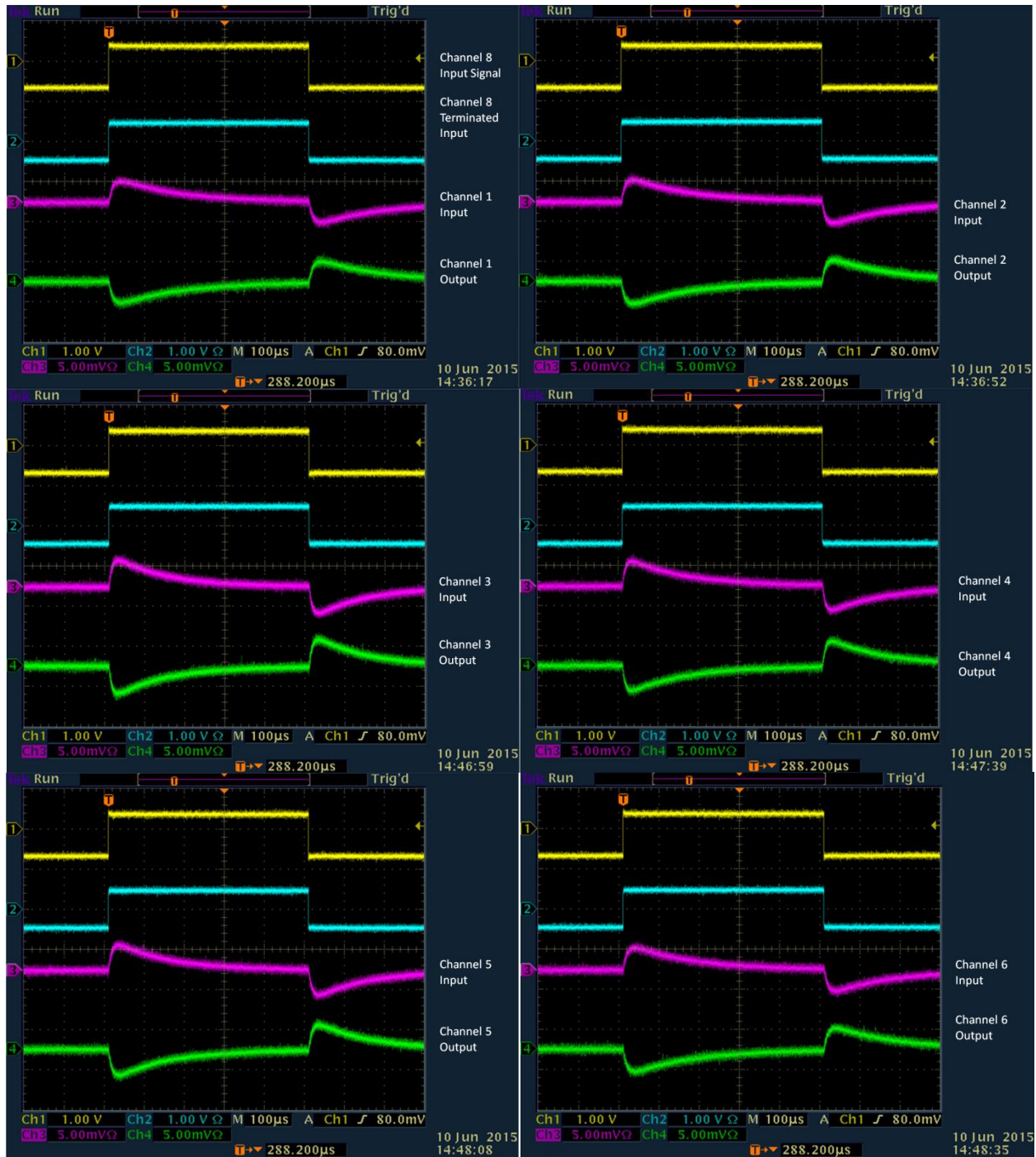


Appendix II - Coaxial Cables Cross Talk Images

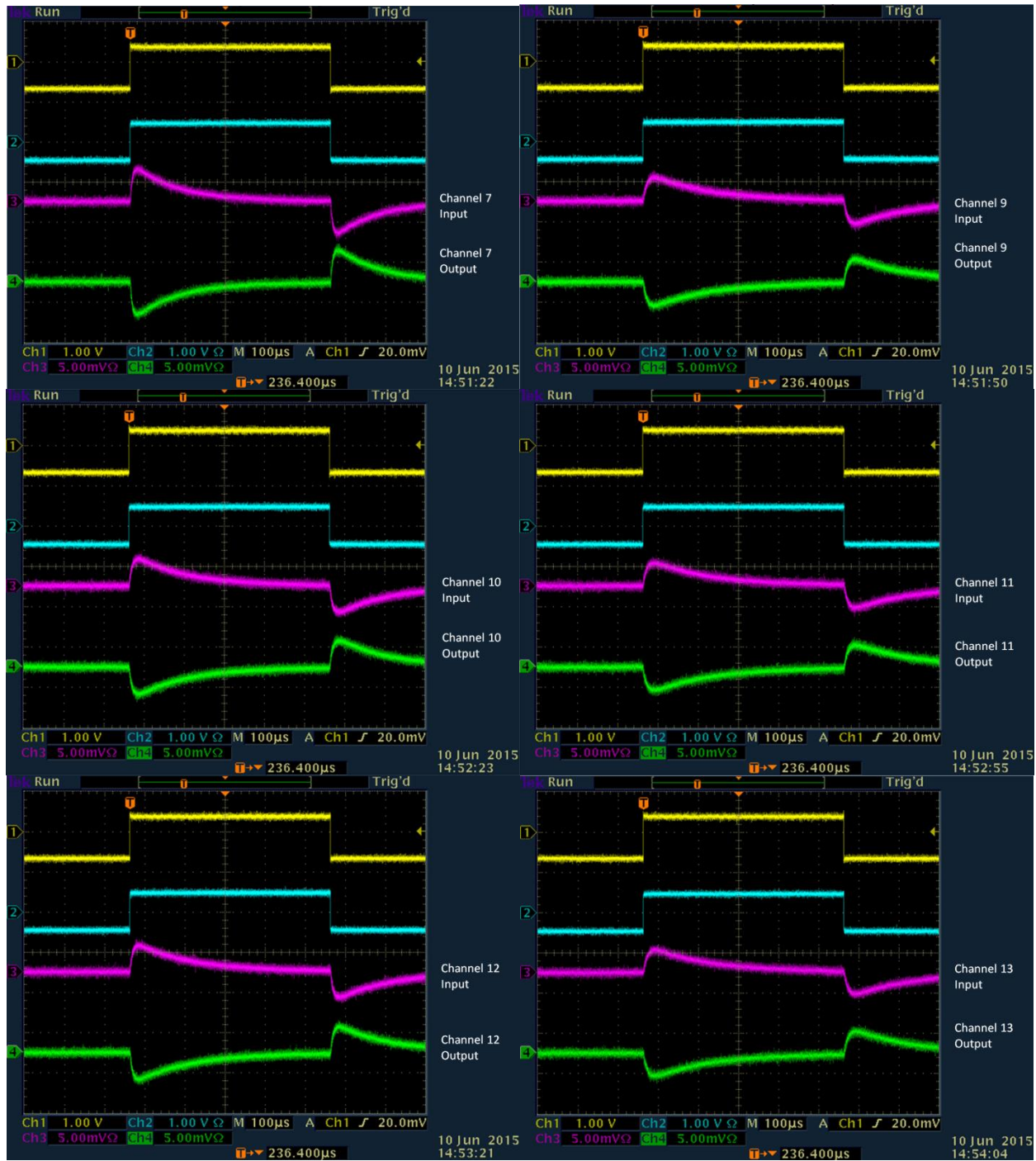


Appendix II - Coaxial Cables Cross Talk Images

Channel 8 Cross Talk Images



Appendix II - Coaxial Cables Cross Talk Images

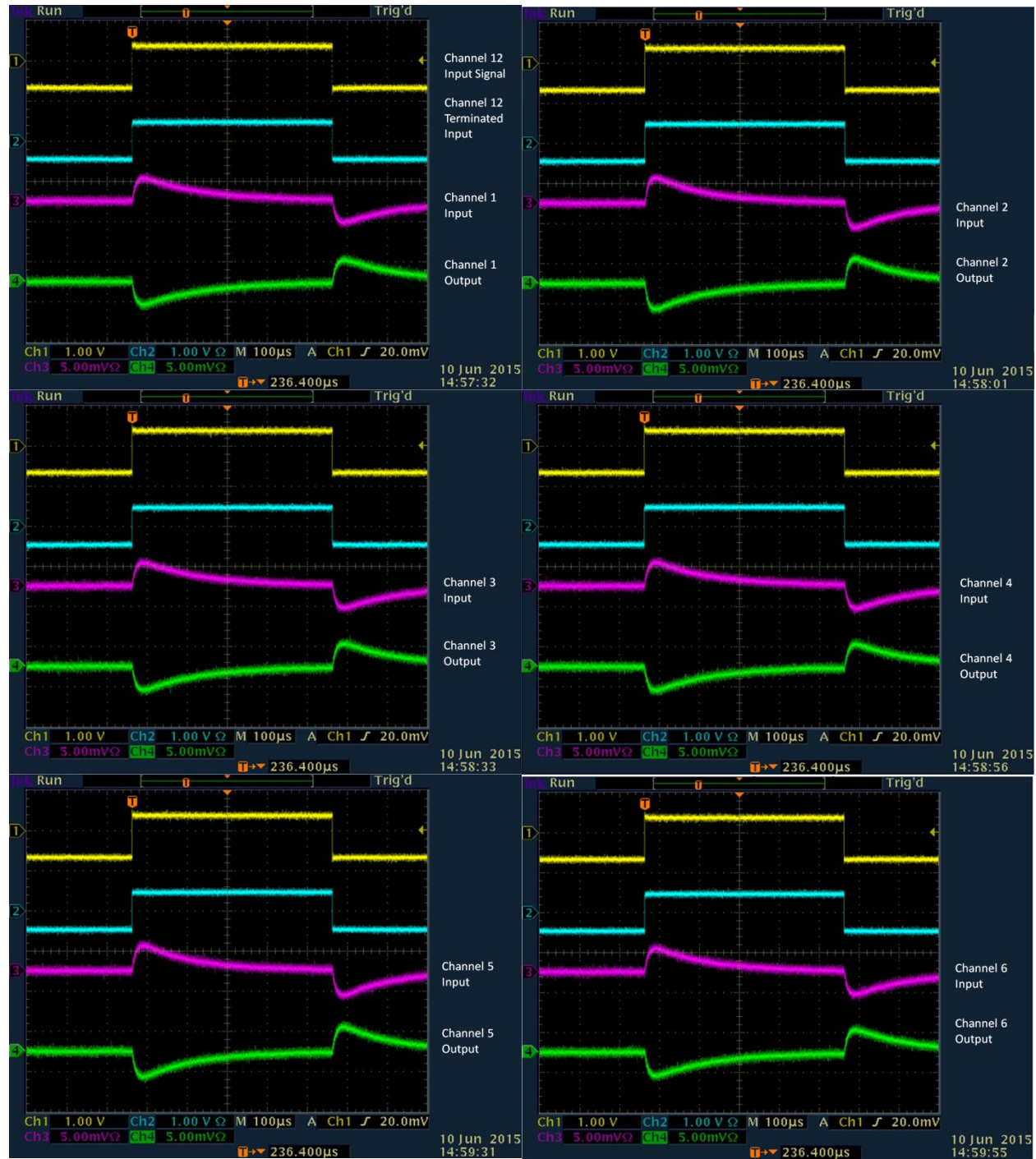


Appendix II - Coaxial Cables Cross Talk Images

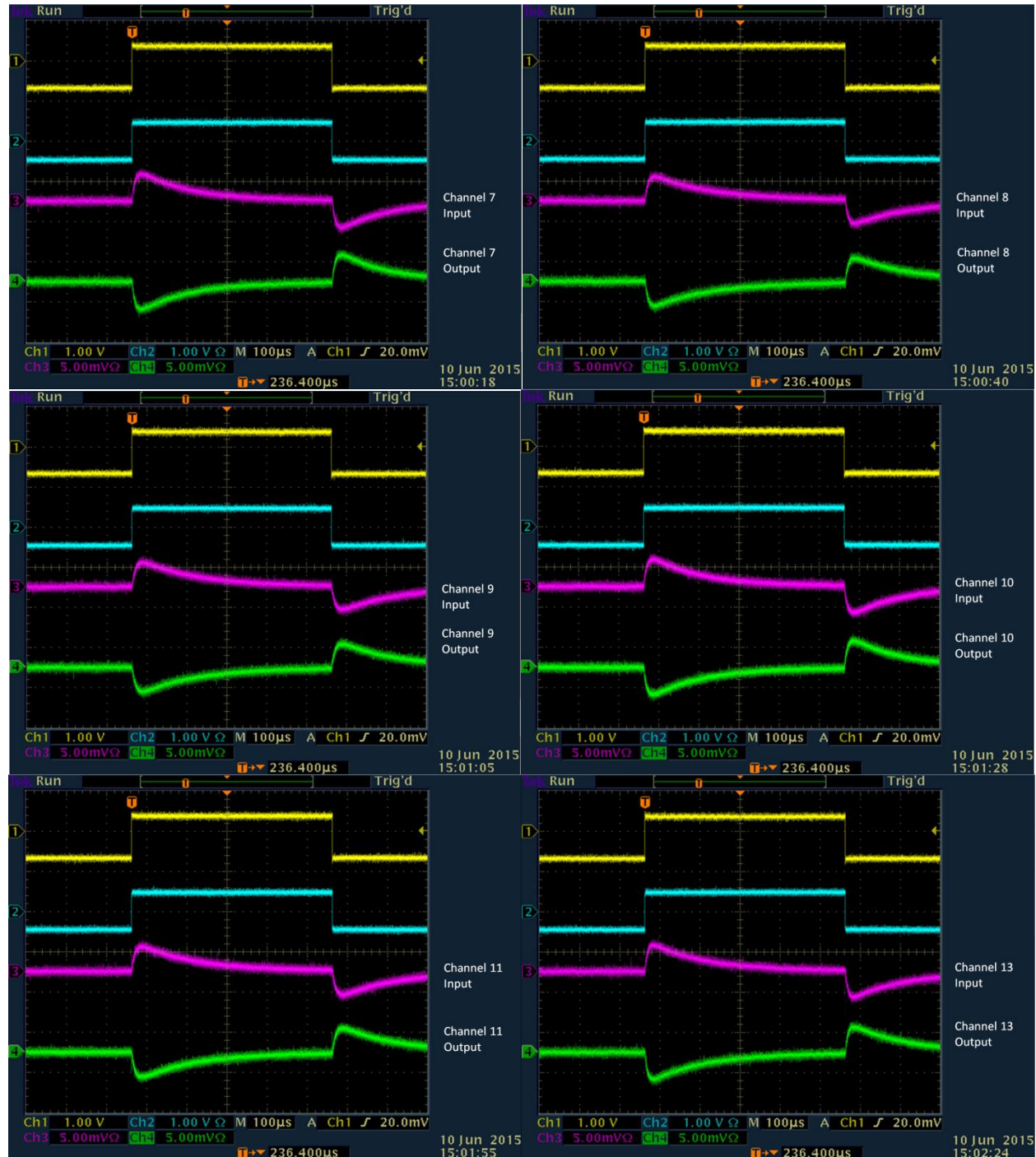


Appendix II - Coaxial Cables Cross Talk Images

Channel 12 Cross Talk Images



Appendix II - Coaxial Cables Cross Talk Images

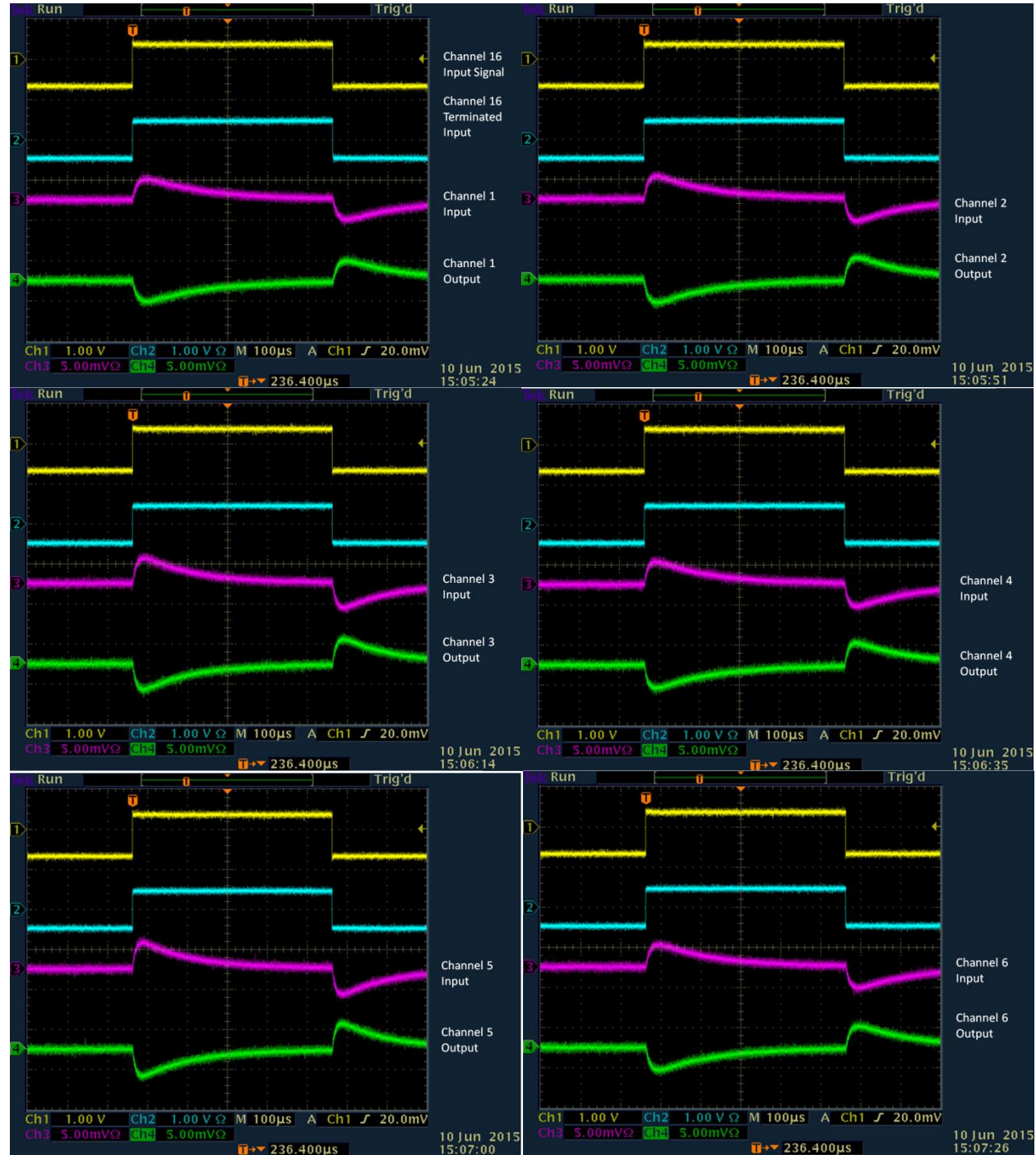


Appendix II - Coaxial Cables Cross Talk Images

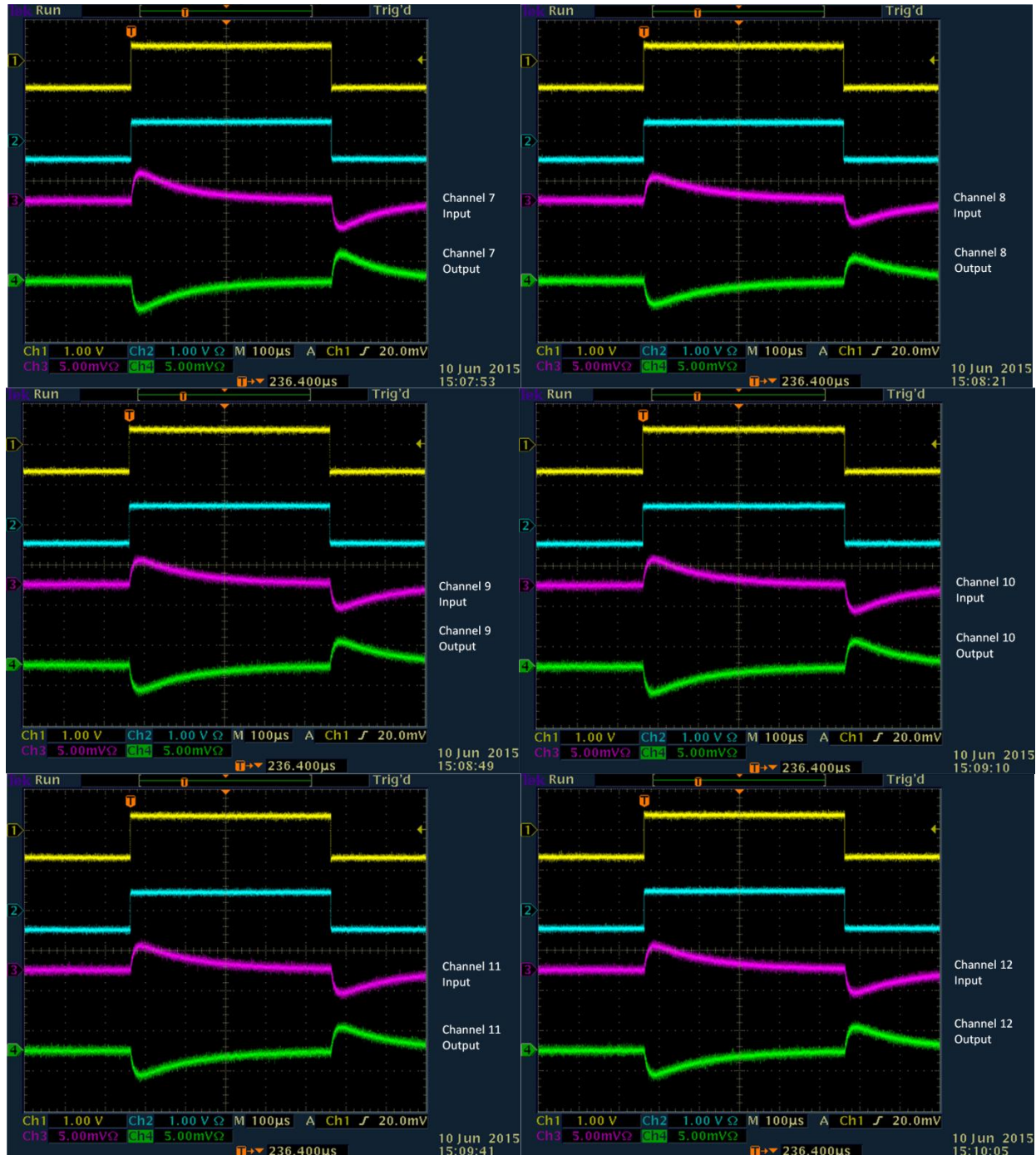


Appendix II - Coaxial Cables Cross Talk Images

Channel 16 Cross Talk Images



Appendix II - Coaxial Cables Cross Talk Images



Appendix II - Coaxial Cables Cross Talk Images

